

Anexos

Projeto Universal FAPESC 2024

Proponente Adriano Fagali de Souza

GPCAM/UFSC

- 1) Cartas de apoio ao projeto

- 2) Geometria do corpo de provas e o molde que será utilizado

CARTA DE APOIO

À
ADRIANO FAGALI

A empresa WEEE|DO manifesta apoio institucional no desenvolvimento do projeto: “Desenvolvimento científico e tecnológico para utilizar polipropileno reciclado na fabricação de peças com elevado valor agregado”, a ser desenvolvido na Universidade Federal de Santa Catarina – UFSC, coordenado pelo professor Adriano Fagali de Souza.

O projeto tem por objetivo desenvolver tecnologias que possibilitem o emprego de matéria-prima reciclada para a fabricação de produtos plásticos de elevada qualidade (propriedades mecânicas, geométricas e estéticas) e valor agregado. Atualmente, por limitações tecnológicas, emprega-se material reciclado para peças simples com baixo valor agregado.

Os temas abordados neste projeto propiciarão inovação e desenvolvimento tecnológico das indústrias do segmento de transformação de plásticos em Santa Catarina e promove o cuidado com o meio ambiente. A WEEE.DO apoia o projeto e se coloca à disposição para colaboração e apoio cabível ao projeto.

Atenciosamente,

Palhoça, 19 de junho de 2024.


Mark J. Rae
Diretor Executivo
CPF: 363.610.328-84

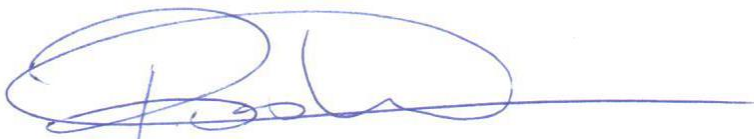
Joinville, julho de 2024

O **Sindicato dos Trabalhadores da Indústria Plástica de Joinville e Região** manifesta apoio institucional no desenvolvimento do projeto: "**Desenvolvimento científico e tecnológico para utilizar polipropileno reciclado na fabricação de peças com elevado valor agregado**", a ser desenvolvido na Universidade Federal de Santa Catarina – UFSC, coordenado pelo professor Adriano Fagali de Souza.

O projeto tem por objetivo desenvolver tecnologias que possibilitem o emprego de matéria-prima reciclada para a fabricação de produtos plásticos de elevada qualidade (propriedades mecânicas, geométricas e estéticas) e valor agregado. Atualmente, por limitações tecnológicas, emprega-se material reciclado para peças simples com baixo valor agregado.

Os temas abordados neste projeto propiciarão inovação e desenvolvimento tecnológico das indústrias do segmento de transformação de plásticos em Santa Catarina e promove o cuidado com o meio ambiente. O **Sindicato dos Trabalhadores da Indústria Plástica de Joinville e Região** tem interesse nos resultados deste trabalho e se coloca à disposição para colaboração e apoio cabível ao projeto.

Atenciosamente,



Presidente

Joinville, julho de 2024

A **Associação Brasileira da Indústria de Ferramentais - ABINFER** manifesta apoio institucional no desenvolvimento do projeto: **"Desenvolvimento científico e tecnológico para utilizar polipropileno reciclado na fabricação de peças com elevado valor agregado"**, a ser desenvolvido na Universidade Federal de Santa Catarina – UFSC, coordenado pelo professor Adriano Fagali de Souza.

O projeto tem por objetivo desenvolver tecnologias que possibilitem o emprego de matéria-prima reciclada para a fabricação de produtos plásticos de elevada qualidade (propriedades mecânicas, geométricas e estéticas) e valor agregado. Atualmente, por limitações tecnológicas, emprega-se material reciclado para peças simples com baixo valor agregado.

Os temas abordados neste projeto propiciarão inovação e desenvolvimento tecnológico das indústrias do segmento de transformação de plásticos em Santa Catarina e promove o cuidado com o meio ambiente. A **EMPRESA** tem interesse nos resultados deste trabalho e se coloca à disposição para colaboração e apoio cabível ao projeto.

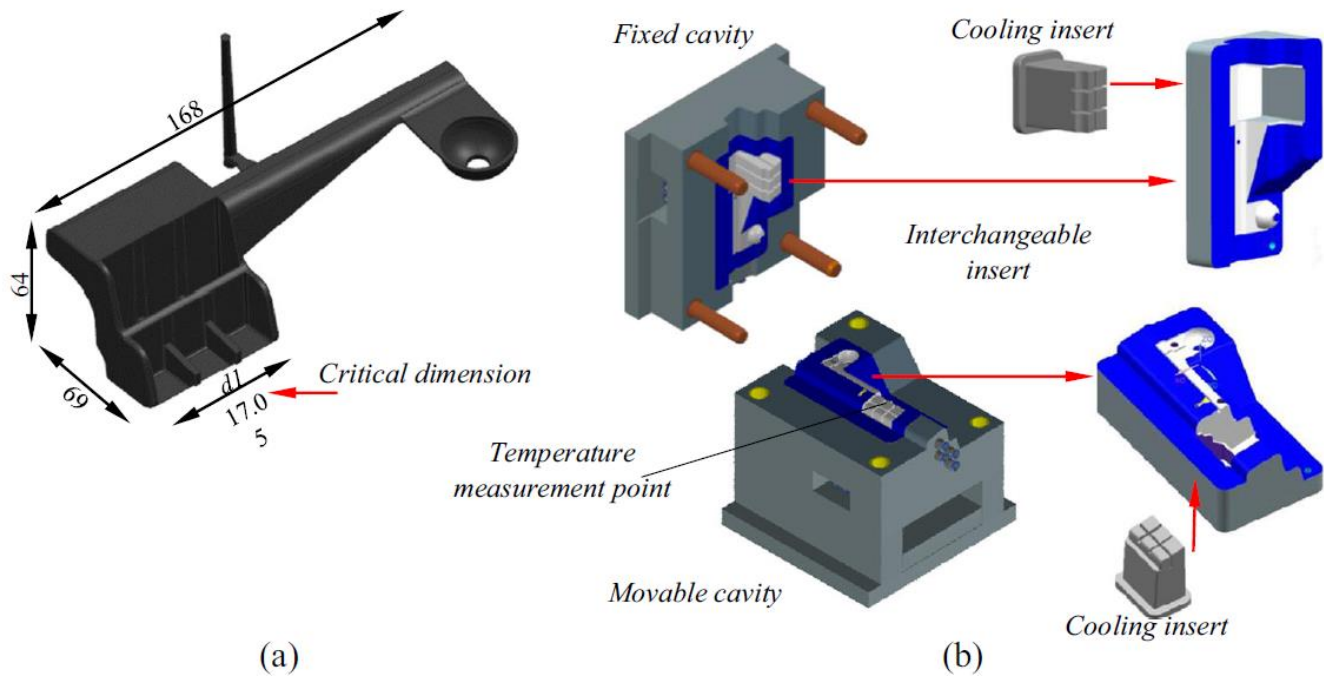
Atenciosamente,

CHRISTIAN
DIHLMANN:49359
720925

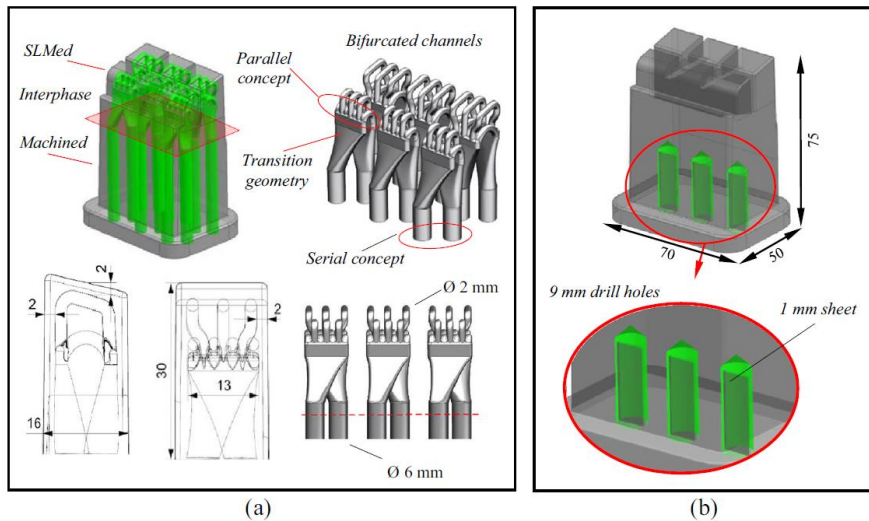
Assinado de forma digital por
CHRISTIAN
DIHLMANN:49359720925
Dados: 2024.06.19 18:07:17
-03'00'

Christian Dihlmann
Presidente ABINFER

Anexo 2



Geometria da peça e projeto do molde



a) Inserto com canais conformados. b) inserto com canais convencionais (Bufile).



Molde com os inserts intercambiáveis – refrigeração convencional e refrigeração conformada



A new hybrid process combining machining and selective laser melting to manufacture an advanced concept of conformal cooling channels for plastic injection molds

Felipe Marin¹ · Adriano Fagali de Souza² · Carlos Henrique Ahrens³ · Luis Norberto López de Lacalle¹

Received: 18 November 2020 / Accepted: 28 January 2021

© The Author(s), under exclusive licence to Springer-Verlag London Ltd. part of Springer Nature 2021

Abstract

Firstly, this work investigates a new design of a conformal cooling channel for injection molding tools containing serial and parallel circuits. Secondly, a hybrid-manufacturing process, combining machining and metal powder additive manufacturing, was also evaluated to manufacture molds. Specimens were manufactured by selective laser melting (SLM) using stainless steel (Corrax®) powder, which was deposited on a pre-machined PH13-8Mo stainless steel substrate. The melting zone interface (MZI) between the two materials were assessed. The results showed that the laser-melted and machined surfaces were successfully melted and bonded. Thus, an injection mold was designed and manufactured. A pair of inserts containing the conformal cooling channels were manufactured by the hybrid process and another equivalent pair of inserts containing a conventional cooling system were produced only by machining. Injection molding was carried out alternating the two types of inserts. The results showed that the mold with the conformal cooling channels reduced the warpage of the injected plastic parts by a factor of ~7. The difference in temperature along the insert was reduced by a factor of ~10 and the molding cycle time was around 36% shorter compared with that of the conventional mold. Overall, the proposed hybrid manufacture of the inserts reduced the manufacturing costs and time by 53% and 60%, respectively. The results indicate the benefits of using the proposed conformal cooling design and the hybrid-manufacturing approach, which combines machining with additive manufacturing for injection mold production.

Keywords Hybrid manufacturing · Additive manufacture · Selective laser melting · Conformal cooling · Injection molding

1 Introduction

Currently, injection molding is the process most used to manufacture plastic components. The plastic molding cycle phases are (a) injection (filling and compression), (b) packing, (c) cooling, and (d) part extraction. During the molding cycle, the molds are cooled by a cooling system consisting of internal channels, through which coolant fluid flows. The cooling phase has a dramatic effect on productivity since it consumes more than two-thirds of production time [1]. The efficiency of

the cooling system in the injection molding process influences both the cycle time and plastic product quality. This step must be as short as possible and able to achieve a homogeneous heat exchange between the plastic part and the mold. Currently, drilling is the conventional way to manufacture the cooling channels and so only straight channels are possible. However, for plastic parts with complex freeform surfaces, straight channel cooling lines can cause non-uniform heat exchange between the plastic and the mold. This decreases the product quality and mold productivity.

To overcome this issue, additive manufacturing by selective laser melting (SLM) has been considered to produce molds containing cooling channels that follow the mold cavity freeform surfaces. This approach is known as conformal cooling.

Because of the high costs of SLM, most studies on conformal cooling have been carried out with the use of numerical simulations. The result obtained shows the benefits of the conformal cooling either from the productivity point of view, as reported by Zheng et al. [2], who reduced the cooling time

✉ Adriano Fagali de Souza
adriano.fagali@ufsc.br

¹ The Aeronautics Advanced Manufacturing Center (CFAA), University of the Basque Country (UPV/EHU), Bilbao, Spain

² Federal University of Santa Catarina (UFSC), Joinville, Brazil

³ Federal University of Santa Catarina (UFSC), Florianópolis, Brazil

by up to 72%, or by improving the quality of the plastic parts, as described by Mohamed et al. [3], who reduced the shrinkage by up to 17%.

However, few experimental scientific studies on molds with the conformal cooling channels manufactured by SLM can be found in the literature. Mazur et al. [4] conducted an investigation of a real mold with the conformal cooling channels in a serial design manufactured by SLM, using H13 steel to mold a plastic box. The results showed that a lower and more homogeneous temperature of the conformal cooling inserts resulted in better plastic parts and reduced the cycle time. This study was performed using a simple plastic box with symmetric geometry (i.e., without geometric complexity) as the workpiece.

Abbès et al. [5] investigated the molding process using a mold with conformal cooling to produce parts of a real automotive component with more complex geometry. However, the design of the cooling channels is simpler, using linear circuits without bifurcations, arranged in a serial design. The authors applied the concept of hybrid molds by assembling parts manufactured by SLM along with parts manufactured by machining. Even though the SLM part was manufactured using maraging steel, which has a lower thermal conductivity, the mold with conformal cooling presented a reduction of 65% in the molding cycle time.

Park and Dang [6] performed an investigation using a mold with conformal cooling for an automotive part with complex geometry. The channels were designed in a spiral and also arranged in a serial design without bifurcations. The authors used P21 steel to manufacture the mold insert by SLM. In this case, the molding cycle time was reduced by 23%.

Based on a review of the literature, it can be noted that more than two decades of research have been carried out in the field of conformal cooling and additive manufacturing for injection molding. Most analyses involve simulation using commercial software or alternative proposed methods. Although some authors investigated the performance of the conformal cooling system experimentally, most of them studied plastic parts with simple geometries, such as plates, boxes, and shell bodies, and the inserts of the molds were manufactured entirely by the SLM process. The hybrid-manufacturing approach (machining and SLM) has not been investigated and is not well understood.

The hybrid-manufacturing concept, combining machining (regions with simple shapes) and SLM (regions with complex shapes), could be a promising alternative to reduce SLM costs and the time required to manufacture injection molds. The results reported herein lend support to a new trend in relation to machine conception, with both manufacturing techniques (machining and SLM) applied in a single machine structure, as described by Liu et al. [7].

Herein, a new design of conformal cooling, mixing serial and parallel cooling circuits, using bifurcated channels, is

proposed and investigated. An injection mold was manufactured applying the hybrid-manufacturing concept. The efficiency of the proposed conformal cooling system is compared to a conventional baffle cooling system when applied to inject a complex automotive part. The injection process and the plastic parts are investigated as well as the main mechanical properties of the metal parts manufactured by the hybrid process.

2 Background

2.1 Design of molds with conformal cooling

The design of conformal cooling systems involves the definition of channel dimension, position, and the layout of the feed systems (parallel or serial). Figure 1 shows the geometrical parameters that need to be considered for a circular cross-sectional channel.

Based on the parameters in Fig. 1, Table 1 shows the values used by different authors to design cooling channels.

The parameters presented in Table 1 are some suggestion guides for designing cooling channels. Depending on the part's geometry, it might be not convenient to follow these parameters, because of either the dimension limits or the geometric shape. Thus, some alterations can be necessary.

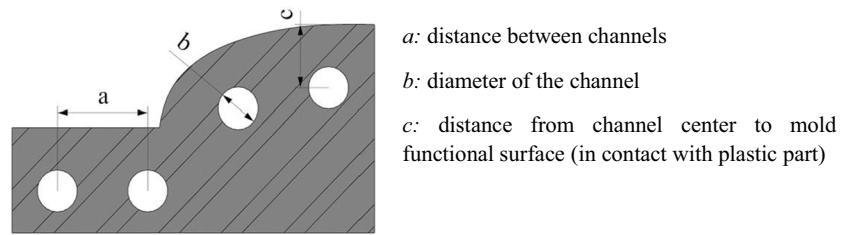
With regard to the design of conformal cooling systems, Marques et al. [12] used commercial simulation software to evaluate the design of either serial or parallel circuits. The results showed that serial circuits had better heat exchange and a more uniform coolant flow rate when compared to parallel circuits, which presented uneven turbulence and regions with lower heat exchange. Wang, Yu, and Wang [13] showed that serial conformal cooling was more efficient than parallel circuits because of the higher flow rate. Marin, Miranda, and Souza [8] investigated the combination of serial and parallel circuits by numerical simulation where the parallel circuit was applied in critical areas and serial circuits elsewhere, keeping the coolant flow rate as constant as possible and improving the heat exchange, without evaluations of cost and the manufacturing process.

2.2 Thermal analysis of molds with conformal cooling

A general background about the heat transfer process and the conditions that drive the injection molding is presented ahead. It is convenient to understand the co-relations among the parameters to better understand the process and the design of a mold.

According to Xu et al. [14], Eq. (1) can be considered to evaluate the heat transfer between the coolant, mold, and hot plastic and to determine the balance of energy at the advancing front of the polymer, considering an adiabatic boundary.

Fig. 1 Geometrical parameters for conformal cooling



a: distance between channels
b: diameter of the channel
c: distance from channel center to mold functional surface (in contact with plastic part)

$$\Delta E = E_{in} - E_{out} + E_g \tag{1}$$

where ΔE is the energy variation, E_{in} is the energy entering, E_{out} is the energy exiting, and E_g is the energy generated in the control volume. According to Park and Dang [6], when the heat balance is established, the heat flux supplied from the plastic part to the mold and the heat flux removed from the mold by the coolant are in equilibrium. Thus, the heat balance can be expressed by Eq. (2) as,

$$Q_m + Q_c + Q_e = 0 \tag{2}$$

where Q_m is the heat flux related to the melted polymer, Q_c is the heat flux provided by the coolant, and Q_e is the external exchange with the surrounding environment. From the balance of energy, the thermal conditions at the advancing front of the polymer can be analyzed using the equivalent thermal circuit shown in Fig. 2. Thus, considering the thermal circuit representation (Fig. 2), the influence of the distance from the coolant channel to the mold surface (dimension l) is expressed by Eq. (3),

$$q'_{cond} = -k \frac{(T_2 - T_1)}{l} \tag{3}$$

where q'_{cond} is the heat flux, k is the thermal constant, and $T_2 - T_1$ is the temperature difference between the mold functional surface and the cooling channel.

Equation (3) shows that the heat exchange increases when l decreases. However, it also implies a reduction in the mold

wall thickness, which would reduce the mold strength. The transient evaluation can be performed based on the thermal diffusivity in polymers. On analyzing heat losses from the sample surfaces using the finite difference scheme, the thermal diffusivity is governed by Eq. (4) [15],

$$\left(\frac{\partial T}{\partial t}\right) = a \left(\frac{\partial^2 T}{\partial x^2}\right) \tag{4}$$

where t is the time, a is the thermal diffusivity, x is the distance, and T is the temperature.

Correlating Eqs. (1), (2), (3), and (4) and Fig. 2, it is possible to note the behavior of the heat flux and the mold wall temperature against the distance between the cooling channels and the mold wall, so it can help designers to go forward with the parameters presented in Table 1, taking into account the limitations of the material's properties of the mold (i.e., wall thickness – parameter c on Table 1).

In the flow analysis of the bifurcated conformal cooling channels arranged as parallel circuits, the effect of the flow bifurcations must be taken into account even considering the fluid as incompressible. Thus, the mass, momentum, and energy conservation are considered, as described by Eqs. (5), (6), and (7), respectively [16, 17].

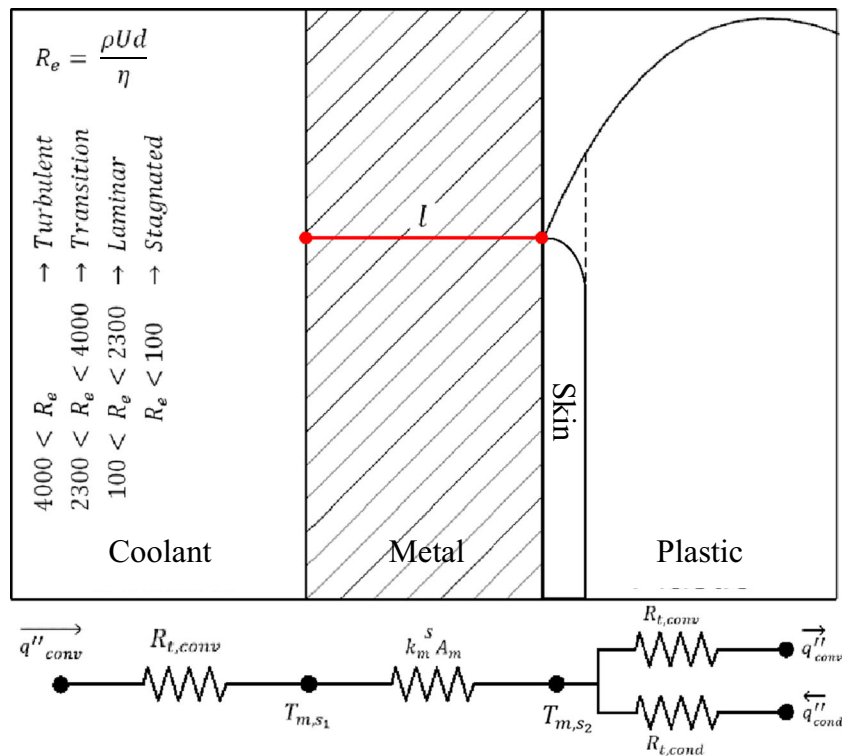
$$\text{Mass } \frac{\partial \rho}{\partial t} + (\nabla \cdot \rho v) = 0 \tag{5}$$

$$\text{Momentum } \rho \frac{\partial v}{\partial t} = -\nabla \cdot \rho + [\nabla \cdot \eta \dot{\gamma}] - \rho [v \cdot \nabla v] \tag{6}$$

Table 1 Dimensions used by some researchers to design cooling channels [8]

| Author | Wall thickness (mm) | Channel diameter (mm) - <i>b</i> | Distance between channels (mm) - <i>a</i> | Channel left to mold surface (mm) - <i>c</i> |
|--------------------|---------------------|----------------------------------|---|--|
| Dang and Park [9] | 2 | 8–10 | $c = 0.7a + 1.6b$ | |
| | 2–4 | 10–12 | | |
| | 4–6 | 10–14 | | |
| Mayer [10] | 0–2 | 4–8 | $2b \leq a \leq 3b$ | $1.5b \leq a \leq 2b$ |
| | 2–4 | 8–12 | | |
| | 4–6 | 12–14 | | |
| Park and Pham [11] | - | 6–12 | $2b \leq a \leq 5b$ | $b \leq c \leq 5b$ |

Fig. 2 Equivalent thermal circuit analysis



$$\text{Energy } \rho \cdot C_p \left(\frac{\partial T}{\partial t} + v \cdot \nabla T \right) = \beta T \left(\frac{\partial p}{\partial t} + v \cdot \nabla p \right) + \eta \gamma^2 + \nabla \cdot (k \nabla T) \quad (7)$$

Clemente and Panão [18] proposed a mathematical method that considers the minimization of the flow resistance when designing a conformal cooling circuit containing bifurcated channels. Using Eqs. (5), (6), and (7), and the Lagrange multipliers method, the authors proposed an equation to minimize the flow resistance for multiple circular cooling channels according to the relation between the primary channel (D_1) and the bifurcated secondary channel (D_2) described as:

$$\frac{D_1}{D_2} = n^{1/3} \quad (8)$$

where n is the number of bifurcated channels. Equation (9) gives the maximum number of channels that maximizes the heat transfer, respecting a minimum distance between the secondary channels (D_2),

$$n_{\max} = \text{floor} \left[\frac{\pi L_1 \tan(\alpha)}{D_2} \right] \quad (9)$$

where $\text{floor}[x]$ is set to the nearest integer value less than or equal to x , L_1 is the segment of the channel, and α is the angle between the primary and bifurcated channels [18]. Increasing the number of secondary channels increases internal

turbulence. The Reynolds number (Re) quantifies the flow turbulence, that is, an increase in Re means that there is an increase in the circuit efficiency [12]. The control of Re in conventional straight drilled cooling channels is easier than in circuits with several bifurcations, as is the case of parallel circuits that require more volume of coolant [11]. The proposed conformal cooling design developed in the current work follows the Clemente and Panão [18] constraints.

2.3 Manufacture of molds with conformal cooling

Firstly, considering simple geometries of the plastic parts, such as planar shapes, it is possible to manufacture the conformal cooling channels only by machining. The mold inserts

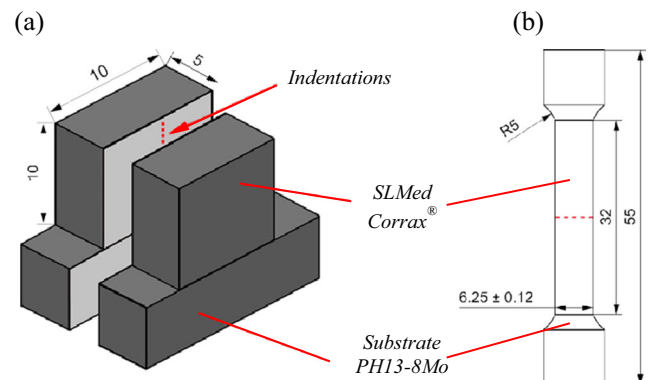


Fig. 3 Specimens manufactured applying the hybrid concept. **a** Prismatic geometry used to analyze the hardness, density, and the melted zone. **b** ASTM 370 specimen used for tensile tests

Table 2 SLM parameters for Corrax®

| SLM process | |
|---------------------------|-------------------------|
| Atmosphere | Nitrogen |
| Laser power | 400 W |
| Layer thickness | 45 μm |
| Overlap | 30% |
| Hatch | 105 μm |
| Laser speed | 1240 mm/s |
| Volumetric energy density | 68.27 J/mm ³ |

must be divided into two sections, each one containing half of the cooling channel path. These sections are then assembled and sealed with O-rings [19]. This is a low-cost solution to reach good heat exchange in the mold. However, this method is extremely limited for most real applications.

Another concept involves the use of hybrid molds, where the inserts of the molds are manufactured by different processes, as in the studies mentioned in Section 1, where some components of the mold were manufactured by machining and others by additive manufacturing [5, 6, 20, and].

In conventional SLM manufacturing, the part is built on a substrate plate. After manufacturing, the part is removed from the substrate by cutting.

Today, mold cavities can be manufactured by means of SLM in high hardness materials with low porosity and high mechanical properties [21]. In SLM, energy density is an important factor, along with the laser power, scanning speed, layer thickness, powder quality, and printing direction, all of which are related to the final material porosity and mechanical properties [22]. The effect of porosity and internal voids on the mechanical properties is clear, but porosity also affects the thermal properties of the mold [23]. The thermal heat transfer is

probably lower, due to the anisotropy nature of the additive manufacturing process in comparison with material produced by cold rolling or forging [24].

Laser-based processes produce a melted zone interface (MZI) between the substrate/layer and deposited material, which results in a heat-affected zone that can influence the mechanical performance of the manufactured part. Since high-temperature gradients are involved, residual stresses and cracks can occur, which creates problems for the manufacture of high-quality parts [25]. At the beginning of the SLM process, considering the substrate at room temperature, there is a large temperature difference between the first layers of the SLM and the substrate.

The study reported herein introduces a new concept of hybrid manufacturing of the inserts. Initially, the region of the inserts with a simple geometry is manufactured by machining. The complex regions of the inserts (with the conformal cooling channels) are then manufactured by SLM, using the machined part as the substrate. Thus, the volume produced by SLM can be reduced, as well as costs and manufacturing time. However, two constraints must be considered: (i) It is difficult to ensure efficient bonding in the powder bed fusion with the substrate (which is a fraction of the desired part in the proposed process). This creates an interface zone with a high-temperature gradient (substrate at room temperature and high temperature of first layers of the SLM); and (ii) the characteristics of the ordinary SLM process after building the first layers, with a low gradient but with high temperature.

3 Experimental procedure

This study was focused on two objectives. Firstly, the hybrid-manufacturing process, combining machining and metal powder additive manufacturing, was explored with the

Fig. 4 **a** Corrax® powder particles. **b** Powder particle size distribution

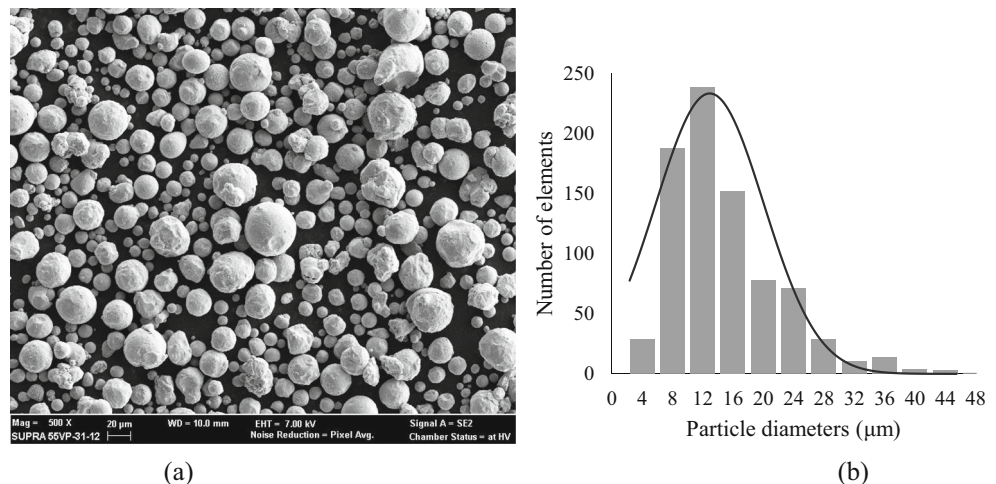
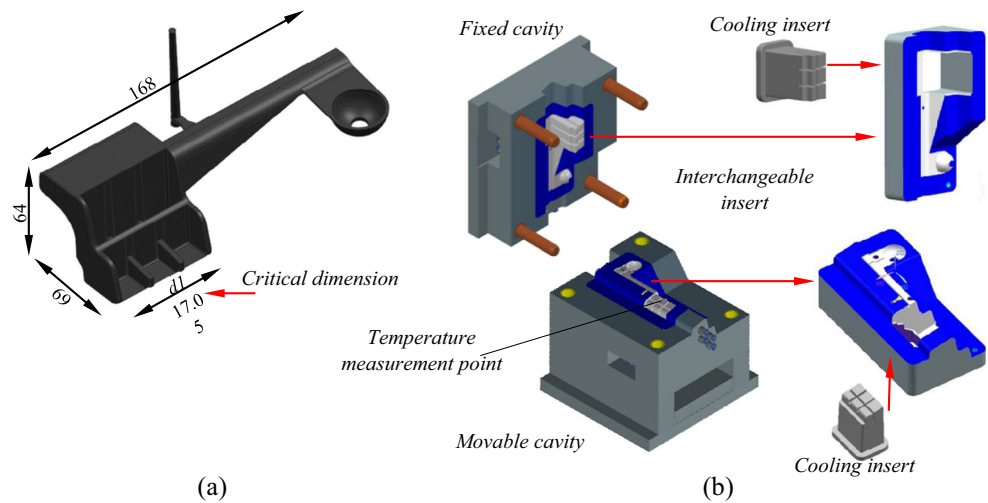


Fig. 5 CAD designs for **a** workpiece and critical dimension d_1 and **b** modular mold and inserts



manufacturing of inserts for injection molds. Secondly, a new design of the conformal cooling channels for injection molding, containing serial, parallel, and bifurcated circuits, was proposed and investigated.

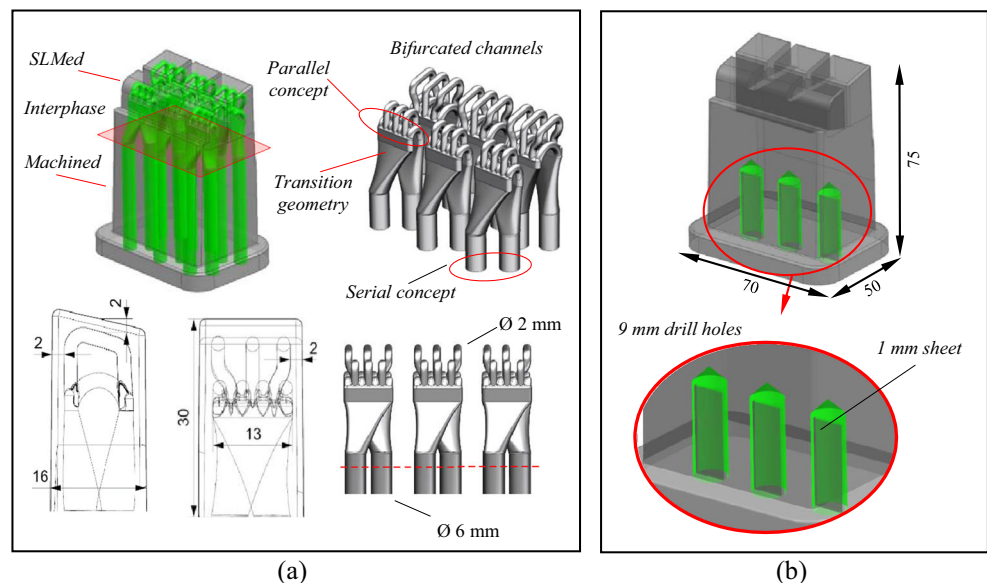
Initially, the mechanical properties of specimens produced by the hybrid-manufacturing process were evaluated. An injection mold was then designed and manufactured. The designed mold contains a pair of exchangeable inserts (for the fixed and movable parts of the mold). Thus, one pair was manufactured applying the new hybrid concept (with conformal cooling) and another pair of inserts with the conventional cooling system (baffle) was manufactured by conventional machining. Evaluations were conducted through CAE simulations and by the experimental plastic injection process, first using the conformal cooling inserts and then using their counterparts with the conventional cooling system. The plastic parts and the molding process were analyzed.

3.1 Evaluating the mechanical properties of the specimens manufactured by the hybrid process

Specimens with two different geometries (prismatic and cylindrical) were manufactured by the hybrid process. In each case, half of the specimen was manufactured by machining and the other half by SLM. The quality of the MZI between SLMed and machined parts was investigated.

An SLM Concept Laser® machine (model CL50WS) with a YAG fiber laser (400 W), a spot size of 100 μm and a laser wavelength of 1064–1070 nm, was used to manufacture all of the SLM parts. Corrax® stainless steel (C 0.03%, Cr 12%, and Ni 9.2%) powder was used in the SLM process and fused onto a pre-machined substrate. Because of commercial restrictions, it was not possible to acquire solid blocks of Corrax® stainless steel processed by conventional rolling.

Fig. 6 Sketches of the exchangeable inserts. **a** Insert with the new bifurcated conformal cooling approach. **b** Insert with a baffle



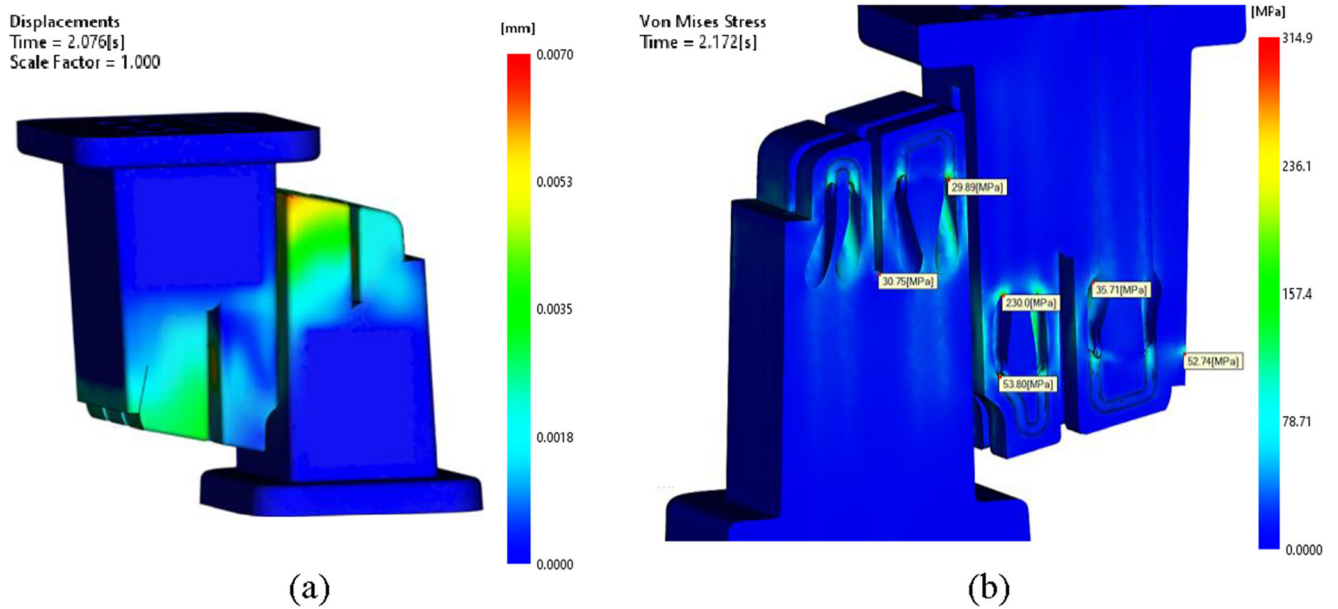


Fig. 7 Simulated **a** maximum displacement and **b** Von Mises Stress at the packing stage

Therefore, solid blocks of martensitic stainless steel PH13-8Mo (13Cr-8Ni-2Mo-1Al-UNS S13800/WNr. 1.4534) produced by the cold rolling process were used as the substrate.

The prismatic specimens (Fig. 3a) and a replica were manufactured by the hybrid process. The porosity was evaluated using metallographic images and the software Multiphase Grains Graphite. The images were taken within 50 μm from the border of the specimens (total of 28 images randomly).

The distribution of the pores was evaluated using a Zeiss® X-ray tomograph (METROTOM 1500) aided by the software Volume Graphics GmbH 3.2. To ensure sufficient penetration of the X-rays, the specimens were cut into four parts.

The hardness was analyzed along the cross section of the specimens with a Wilson Instruments® testing machine (402MVD) according to ISO 6507-1:2008. The hardness profiles of the SLMed and machined portions were

accessed, as well as the melted zone. This zone was also investigated based on images obtained from a Carl Zeiss® stereoscope (Discovery V8).

A cylindrical specimen and one replica were manufactured applying the hybrid process for the tensile testing following the standard ASTM 370 (Fig. 3b) using an Instron® universal testing machine (model 5988).

The SLM parameters applied were recommended by the SLM machine supplier and are shown in Table 2.

The geometry and diameter of the powder particles used were evaluated by scanning electron microscopy (SEM) on a Zeiss® SUPRA 55-VP microscope, with ×500 magnification. Figure 4 shows the particle shape and the distribution of particle diameters. It can be observed that the particle sizes ranged from 5 to 50 μm (Fig. 4a), and the Gaussian curve (Fig. 4b) shows an appropriate distribution for powder packing during the SLM process.

Fig. 8 Manufacture of hybrid mold inserts. **a** Substrates on the SLM table. **b** SLM process. **c** Insert after SLM process

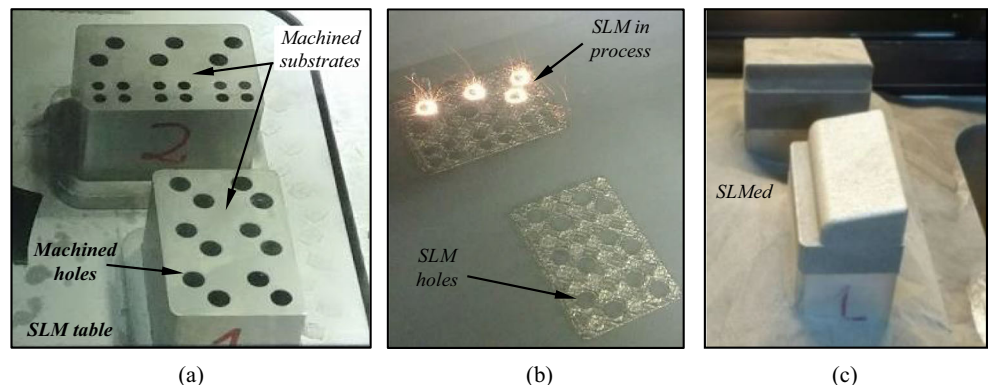
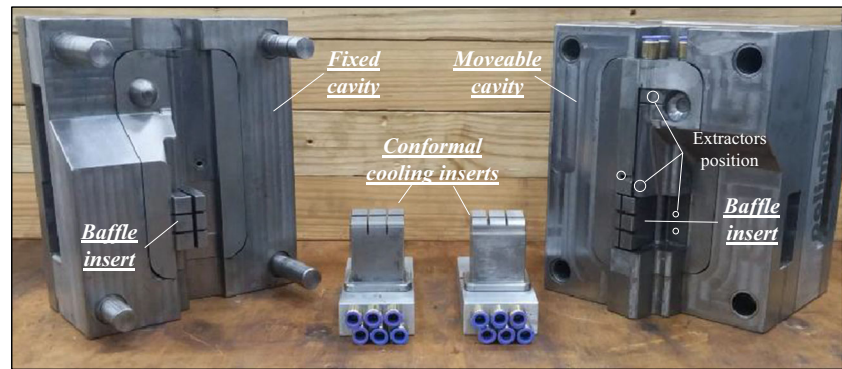


Fig. 9 Mold cavities and the exchangeable inserts (baffle and conformal cooling)



3.2 New approach for conformal cooling design

3.2.1 Design, simulation, and manufacturing of the inserts of the mold

To achieve the objectives of this study, an automotive plastic part was chosen as the workpiece (Fig. 5a). The plastic part was designed with draft angles and ribs considering movable and fixed cavities. It was intended to propitiate more interference with the movable cavity of the mold during the solidification of the part. Thus, when the mold was opened, the part moved together to the movable cavity. After that, the extractors on the movable cavity removed the plastic part from the cavity to finish the injection cycle.

The injection mold was designed with two exchangeable inserts, one for each side of the mold cavity (one fixed and the other moveable), as detailed in Fig. 5b.

One pair of inserts had a conventional cooling system (baffle concept) and was manufactured by machining. The other pair of inserts containing the conformal cooling channels was manufactured by the hybrid-manufacturing approach (machining and SLM). The bottom portion of these inserts has only straight-line holes, which were manufactured by machining (around 2/3 of the insert volume). The top portion of the inserts containing the conformal cooling channels was

manufactured by SLM using the machined portion as the substrate (where the conformal cooling was designed). The same raw materials were used for the hybrid insert and the build parameters are shown in Table 2.

The proposed design for the new conformal cooling system includes a combination of serial and parallel cooling channels, connected by a transition geometry to form a bifurcated circuit. Based on the recommendations in Fig. 1 and Table 1 and taking into account the geometrical constraints of the plastic workpiece, the conformal cooling system was designed using 12 cylindrical channels (6 coolant input and 6 coolant output, the serial component) with a diameter of 6 mm at the bottom of the inserts. Due to the restriction of space at the inserts, each of these channels was split into 5 small channels with diameters of 2 mm (parallel component) using a suave swept with a constant section, as seen in Fig. 6a. The criteria of minimum flow resistance detailed by Clemente and Paño [18] were considered.

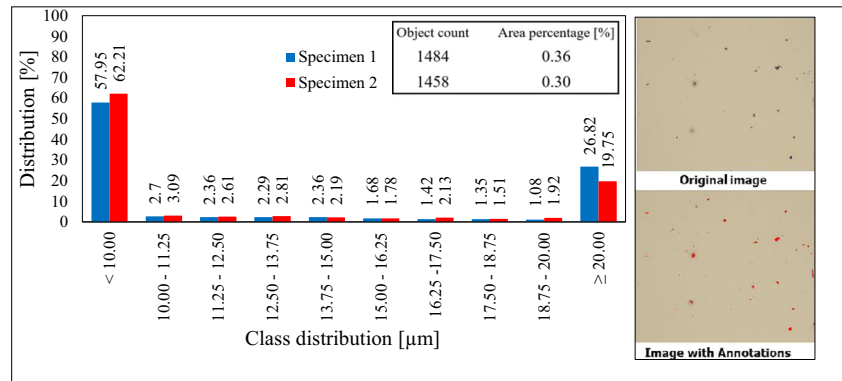
Taking into account Table 1 and aided by CAE simulations, the dimensions a , b , and c were established as 2.1 mm, 2 mm, and 3 mm, respectively. These values were established considering the following aspects:

- i) The dimension a affects the heat transfer homogeneity and it was defined to be the maximum value. But it is

Table 3 Parameters used in simulation and real process

| Injection parameters | |
|--------------------------|---|
| Material | Polypropylene Braskem® grade H 105 |
| Initial mold temperature | 25°C |
| Injection temperature | 240°C |
| Cycle time | 28 s |
| Open-close time | 5 s |
| Filling time | 0.4 s |
| Switchover | 95% filling |
| Packing | 50% injection pressure decreasing to 0 linearly in 2s |
| Coolant fluid | Water |
| Coolant temperature | 25°C (simulation) |

Fig. 10 Density of the SLMed region analyzed by optical images



- limited by the plastic part geometry. And together with the parameter c , both can affect the resistance of the insert.
- ii) The dimension b was selected based on work presented by Manzur et al. [4], which considers the maximum diameter of cylindrical channels manufactured by SLM.
 - iii) The dimension c was selected to maintain a minimum distance from the wall the ensure its mechanical resistance.

The baffle inserts had three channels (diameter 9 mm and length 31 mm) manufactured by drilling (Fig. 6b). One sheet of metal with a thickness of 1 mm was used in each baffle channel.

The baffle and conformal cooling inserts were designed to have the same volume of coolant entering. Both mold configurations were simulated using the CAE software Sigmasoft® 5.1.

The mechanical resistance of the conformal cooling inserts was evaluated. To determine the dimension c (resistance of the inserts), simple estimation analyses were carried out by CAE simulation. First, the injection pressure was obtained (about 32 MPa). Then, the mechanical resistance of the conformal cooling inserts was estimated, considering $c = 2$ mm of wall thickness, Corrax® (material of the inserts), and the geometry of the channels. The results show the maximum displacement of the inserts was 0.007 mm, estimated by the CAE (Von Mises Stress was 314.8 MPa). It is 3 times lower than the maximum resistance of the Uddeholm Corrax® (1100 MPa). Therefore, the inserts were considered to be manufactured. Figure 7 presents the simulations of these displacements and mechanical stress in the packing phase.

Figure 8 details the manufacturing process of the hybrid insert. During the execution of the experimental procedure,

Fig. 11 X-ray tomography images of samples showing porosity

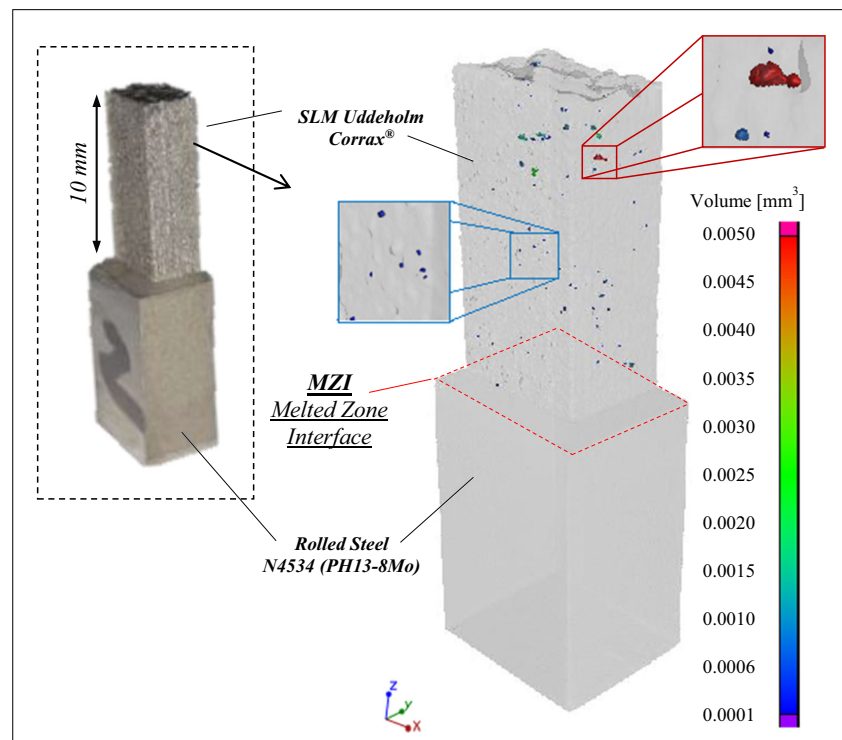
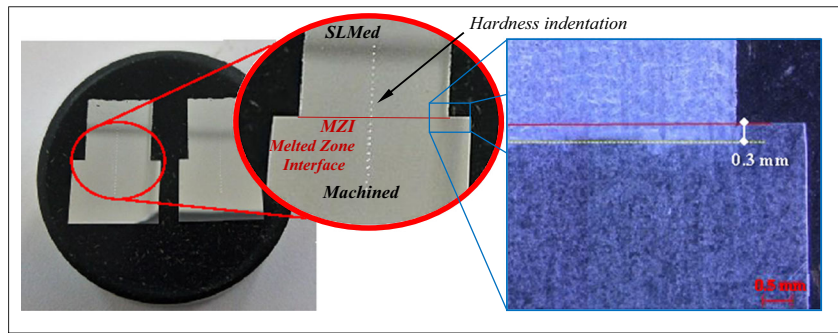


Fig. 12 Depth of MZI and hardness indentations on the machined and SLMed surfaces and at the interface



one important point noted is that the reference coordinate system used for machining the bottom part of the insert and the coordinate system used for the SLM machine to build the top portion of the insert must be accurately aligned. Otherwise, in the SLM process, the channels previously manufactured by machining (Fig. 8a) may be obstructed.

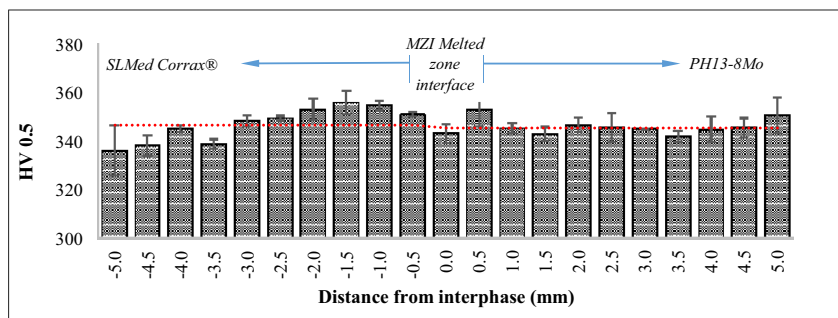
After the SLM, the inserts were finished by milling to achieve accurate surface and roughness according to the end-use requirements. Figure 9 shows the mold cavities manufactured, the interchangeable inserts (baffle assembled and proposed conformal cooling), and also the positions of the extractors of the mold (A-type extractors, two with 9 mm, two with 4 mm, and one with 5 mm of diameter).

3.2.2 Injection molding process and evaluations

Firstly, a batch of plastic parts was produced using conventional inserts with baffle cooling channels. The inserts were then changed to those with the conformal cooling system and the second batch of plastic parts was produced. More than 50 parts were obtained in each batch. The temperature of the mold was verified after each injection cycle using a digital infrared thermometer (KKmoon® GM300), at 300 mm from the top of the movable insert (the temperature measurement point is shown in Fig. 5). A Haitian® MA 2500 injection molding machine cooled with water at 26.1°C (± 2) flowing at 9 l/min was used for the experiments.

The plastic injection molding parameters were obtained from preliminary studies using the CAE software Sigmasoft® 5.1 and are given in Table 3.

Fig. 13 Hardness profile of the hybrid specimens around the melted zone



The quality of the polypropylene (PP) plastic parts was evaluated by means of warpage and form error analysis. An ATOS® (Core 300) scanner and the software ATOS® Professional 2017 were used to compare the scanned and CAD geometries. The critical dimension (d_1) of the injected parts was the focus of the evaluation (Fig. 5a).

4 Results and discussion

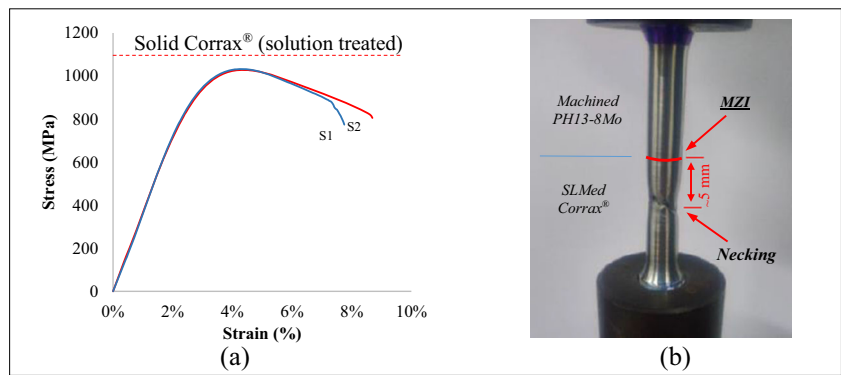
4.1 Mechanical properties of specimens manufactured by the hybrid process

The density of the SLMed region was analyzed using a total of 28 optical images (ten of each specimen) and the software Multiphase Grains Graphite. Figure 10 shows one example of the results obtained.

The density of the specimens considering only the SLM portion reached around 99.7% with a higher concentration of pores with sizes < 10 μm (~60%). The highest percentage of pores (around 60%) were < 10 μm and around 22% were > 20 μm. However, an important factor is the distribution of these pores in the specimen.

Thus, X-ray tomography analysis was carried out and the results in Fig. 11 confirm a low number of pores with most of them being < 0.001 mm³. This reflects the behavior of both constraints of the proposed hybrid manufacturing: (i) the melted interface zone where the powder bed fuses with the substrate, and (ii) the properties of the ordinary SLM process after building the first layers.

Fig. 14 Tensile test results for the hybrid specimens. **a** Stress-strain curve. **b** Local necking in the SLM region



In hybrid manufacturing, the MZI is the region with the highest temperature gradient and this can result in the formation of cracks due to accumulated stress [25]. However, in the current case, Fig. 11 shows that this temperature gradient did not interfere with the quality of the MZI. The first layers of the SLM (corresponding to the melted zone) and the vicinity presented a lower number of pores and no cracks can be observed. This could be because both materials used (powder and substrate) have high weldability [26]. The high presence of aluminum as an alloying element prevents the formation of intergranular austenite during the solidification of the melt pool and subsequent formation of martensitic structures that are responsible for the residual stresses.

On the other hand, it is possible to note in Fig. 11 that as the distance from the MZI increases (beginning of the SLM process), the pore size also increases slightly. After manufacturing the first layers, the substrate together with the previously melted layers has a significant gain in temperature and, consequently, a reduction in the temperature gradient occurs. This increases the temperature of the manufactured part, which can result in material vaporization and entrapment in the melt pool [27, 28], with the formation of pores in the middle/top portion of the specimens (Fig. 11).

Figure 12 shows the stereoscope photo of the MZI between the machined and SLMed materials.

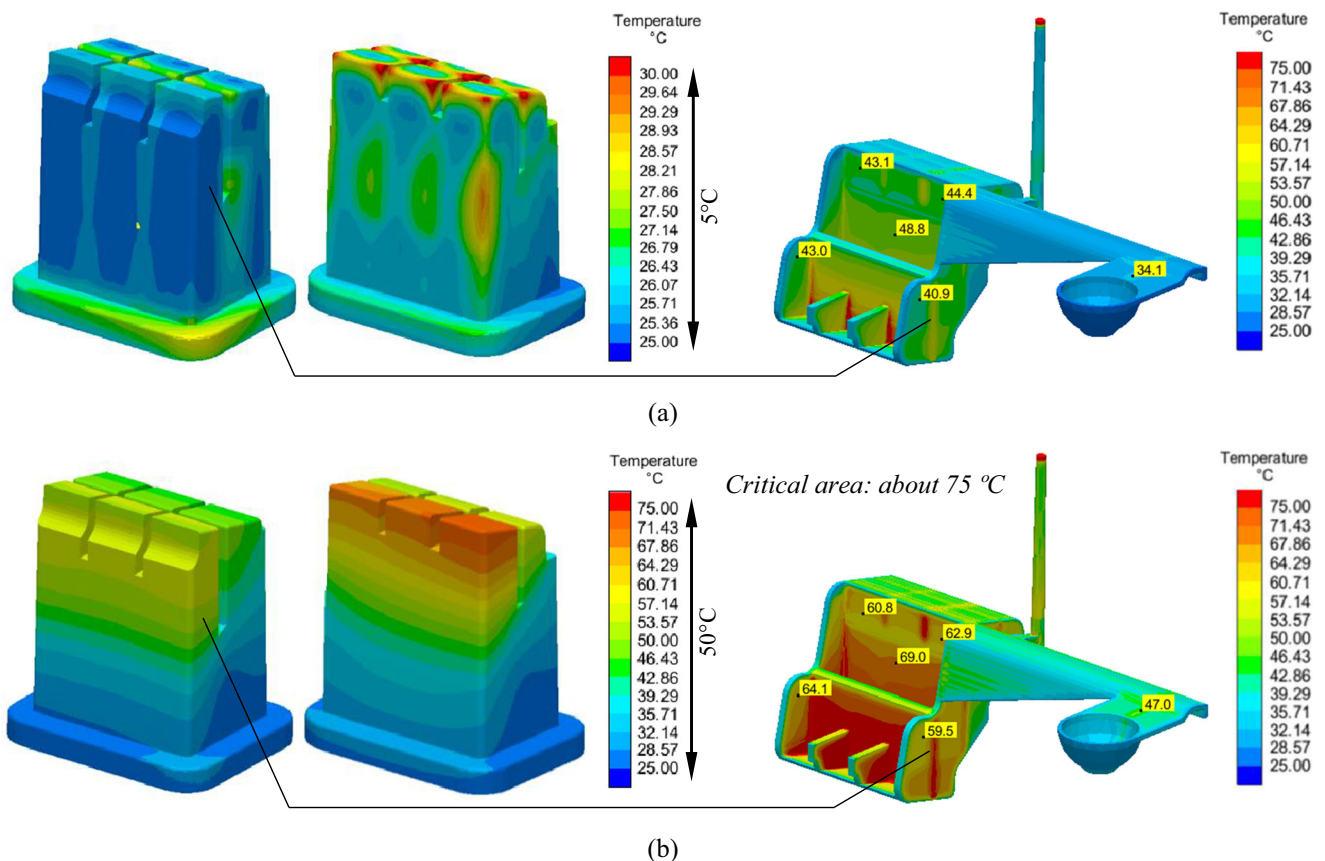


Fig. 15 Analysis of the temperature of plastic parts and inserts (fixed and movable). **a** Proposed conformal cooling inserts. **b** Conventional baffle inserts

Fig. 16 The temperature of the fixed mold inserts measured at the end of the cycle

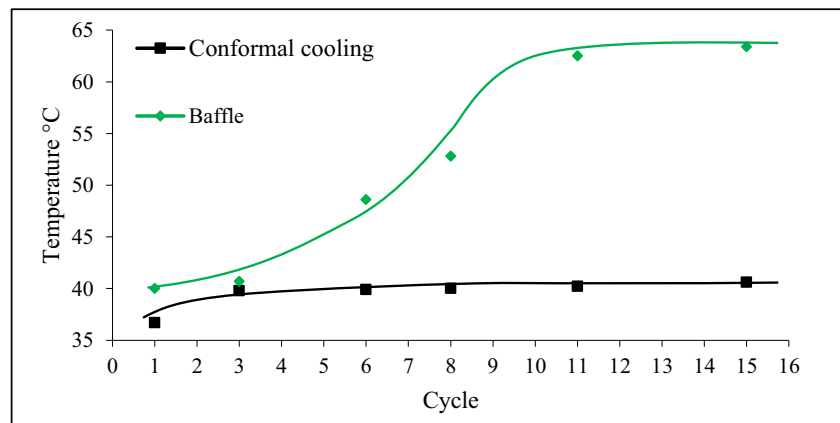


Figure 12 shows that the MZI had a thickness of 0.3 mm and no defects could be detected visually. The analysis was carried out to better understand some of the mechanical properties of this zone. Figure 13 shows the hardness (HV 0.5 ISO 6507-1:2008) values for the MZI (at 0.0 mm), for the SLMed portion (from -0.5 to -5 mm), and the machined portion (from 0.5 to 5 mm). The average hardness was $346 \text{ HV} \pm 6$ (~35 HRC), for values obtained at 21 positions along with the specimens.

The hardness of the cold-rolled PH13-8Mo portion had higher uniformity than the portion manufactured by SLM. After the manufacture of the first layer by SLM, the hardness increases slightly. This phenomenon is because of the rapid solidification of the molten pool that results in the formation of a coarse martensitic structure [28].

The hardness tends to reduce at around 4.5 mm from the MZI on the SLM portion. This is probably due to an increase in the temperature in this region, resulting in a heat-affected zone that possibly underwent high-temperature tempering, which can reduce the strength and the hardness. In addition, this reduction in the hardness may be related to the presence of a greater number of pores, as observed in Fig. 11.

To verify the resistance of the MZI between the SLM portion and the machined substrate, tensile tests were conducted on two ASTM 370 specimens (S1 and a replica S2). A ductile fracture with the formation of necking occurred on the SLM portion (Fig. 14).

The fracture did not occur at the melted zone interface as expected, but around 5 mm from the MZI on the SLM portion, probably due to the higher concentration of pores in this region. This demonstrates that the MZI produced by hybrid manufacturing is not a limitation. Also, it should be noted that the ultimate tensile strength was around 1030 MPa and this value is 7% lower than that of the ordinary rolled solution-treated Corrax® (1100 MPa) [26].

Combining all of the results of this experimental phase, it is possible to draw a close correlation:

- In the portion of the specimens built by SLM, at beyond 5 mm from the MZI, there were more pores present compared with the first layers.
- The hardness of the SLMed portion decreased in this region (around 5 mm after the melted zone).
- The fracture of ASTM 370 specimens occurred at around 5 mm from the melted zone.

Therefore, the results show that in the SLM process, the properties of the specimens altered during their construction. However, there was a relatively small reduction in the ultimate tensile strength together with good mechanical properties in the melted zone. This demonstrates that the proposed hybrid-manufacturing process can be used successfully for many applications. These results

Fig. 17 Dimensional deviation of injected plastic parts. **a** Baffle inserts. **b** Conformal cooling inserts

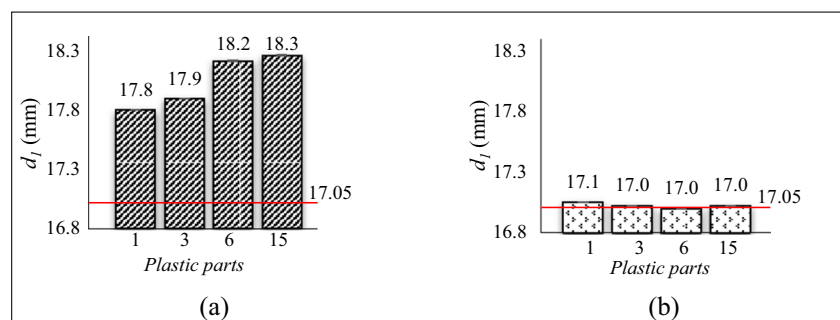
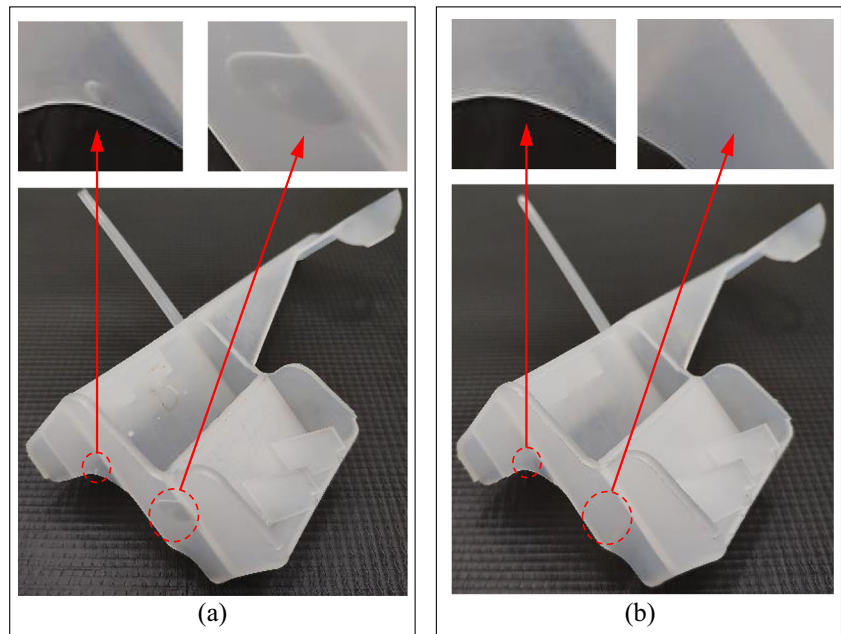


Fig. 18 Visual inspection to identify defects in injected parts produced with **a** baffle inserts and **b** conformal cooling inserts



motivated the continuation of this study and the manufacturing of the injection mold was then carried out.

4.2 Proposed conformal cooling performance evaluation

4.2.1 Simulation analysis

The simulations highlighted the variation in temperature along with the inserts at the end of the cycles. With the same coolant feed flow, the proposed conformal cooling inserts showed better heat exchange efficiency than the conventional baffle cooling, as seen in Fig. 15.

Besides the low values, the conformal cooling inserts led to a high homogeneity in terms of temperature, with a difference between colder and hotter areas of around 5°C. In the case of the baffle inserts, this difference was 10 times higher. This low homogeneity of the conventional baffle inserts could increase the warpage and the deformation of the molded plastic part.

4.2.2 Evaluation of injection molding process and plastic parts

Figure 16 shows the temperature of the mold at the measurement point (Fig. 5), taken with the digital infrared thermometer after the injection cycles, for both cases investigated (baffle and conformal cooling systems). For the mold with baffles, the temperature increased more than 50% (42 to 63°C) from the first cycles up to stabilization (steady-state regime), which was reached after the 11th part produced. These first plastic parts produced are wasted. However, for the mold with conformal cooling, the number of cycles required to reach the steady-state regime is negligible, and the temperature remained constant at around 40°C. This means that the parts tend to have the same quality starting from the first cycles, thus avoiding wastage. Equations (4) to (9) help to understand why the transient regime is different and the homogeneity of the mold differs from conformal cooling to baffle cooling channels, even the cross section on the inlet fluid is the same. Besides these, it correlated to the design parameters of the channels with the efficiency of the bifurcated cooling systems.

Fig. 19 Simulation to enhance the process using the mold with baffle inserts

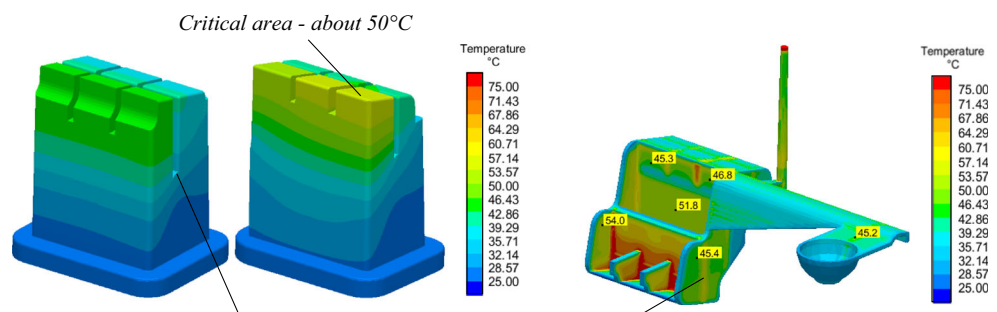


Table 4 Reduction in the SLM volume using hybrid manufacturing

| Insert | Total volume (mm ³) | SLM volume (mm ³) | Machined volume (mm ³) | SLM reduction (%) |
|---------|---------------------------------|-------------------------------|------------------------------------|-------------------|
| Movable | 141.1 | 45.8 | 95.3 | 67.5 |
| Fixed | 156.7 | 51.5 | 105.2 | 67.0 |

Considering the molding process in the steady-state regime, the temperature of the conformal cooling mold was around 40% lower than that of the baffle cooling mold. It is important to mention that the divergence between real and simulated temperatures at the measurement point was low (around 8%).

Besides the difference between the maximum temperatures on the molds, which influences the molding cycle time, the difference in the temperatures along the insert is also important in relation to maintaining the accuracy of the plastic part.

Figure 17 shows the results for the form error of the plastic parts produced using both molds, in the molding cycles 1, 3, 6, and 15. The inspections were carried out considering dimension d_1 (Fig. 5), which is relevant for the plastic component investigated, with a nominal dimension of 17.05 mm. The parts molded using conformal cooling inserts had a d_1 dimension error lower than 1%, whereas the error for the parts molded using the conventional baffle system was around 7% and, depending on the plastic component, this deviation may not be acceptable.

Considering the parts produced in the first cycles (1 to 3) using the baffle inserts, it can be noted that even with a low temperature in these cycles (Fig. 16), close to the conformal cooling temperature, the d_1 dimension errors were significantly higher (Fig. 17a). This is probably because of a greater variation in temperature for the baffle inserts, whereas the variation was negligible for the conformal cooling inserts. The variation in temperature and the d_1 dimension increased non-linearly until the steady-state regime is reached (Fig. 17a and Fig. 16), for the baffle inserts. In this molding regime, the results of the simulation show that the temperature variation in the inserts with baffle reached 50°C, whereas in the conformal cooling system, it was only 5°C. This shows that the conformal cooling promotes an exceptionally small temperature variation along with the inserts, thus reducing the deviations in the part geometry.

Additionally, a visual inspection revealed shrinkage defects and voids in the parts manufactured using the baffle inserts, as seen in Fig. 18a. These defects were not observed in the parts molded with the conformal cooling inserts (Fig. 18b).

The presence of voids was observed in all parts obtained using the baffle inserts, even when the mold was cooler in the initial cycles. This defect did not occur in the parts manufactured using the mold with conformal cooling. The combination of a higher cooling rate in the conformal cooling channel along with the high crystallization rate of the injected material (PP) could hinder the formation of this type of defect.

Additional simulations showed that to obtain plastic parts with a level of quality similar to that obtained with the conformal cooling system, the injection process using the baffle mold would need to be 36% longer, reducing productivity. Figure 19 shows the results of these simulations.

Figure 19 shows that on increasing the cooling time and the total cycle time to 44 s, the homogeneity of the temperature along with the insert increases, and the temperature difference drops to approximately 10°C, which is considered acceptable by injection mold companies [29], and may avoid problems such as warpage and voids. Thus, obtaining injected parts using the baffle inserts would require a longer cycle time compared to conformal cooling inserts. In addition, it is important to note that, besides the longer time required for the manufacturing of each plastic part, all associated expenses, such as energy consumption, labor costs, maintenance of the mold, and the injection molding machine, would also increase.

4.2.3 Simple evaluation of cost and time associated with the hybrid-manufacturing process

To assess the potential for the industrial application of the proposed hybrid-manufacturing process, a simple evaluation of the cost and time involved in the manufacturing of the inserts was carried out (Table 4).

If only SLM is used to manufacture the mold inserts, a cycle time of 38 h would be required. However, using the proposed hybrid-manufacturing approach, the reduction in the SLM volume was around 67% for each insert and the cycle time is reduced to 15 h.

In relation to practical use, the hybrid-manufacturing procedure could reduce the SLM time by around 60% and the costs by around 53% (from an estimated 7500.00 USD to 3500.00 USD considering the current market).

5 Conclusions

This paper describes a hybrid-manufacturing process, combining machining and SLM, to manufacture injection molds and also a new design of the bifurcated conformal cooling channels combining serial and parallel circuits. A real mold was manufactured applying these concepts and a batch of plastic workpieces was produced. The hybrid-manufacturing process, the injection process, and the plastic parts produced were evaluated and the main conclusions are as follows:

- The melted zone interface (MZI)—between the machined and the SLMed portion—can be considered the first constraint of the hybrid-manufacturing process. In the case investigated, the specimens manufactured by the hybrid process had an MZI of 0.3 mm (depth). No defects were observed.
- Contrary to the expectation, the MZI did not lose its mechanical properties, even though a higher temperature gradient occurs in this region (substrate much cooler than initial SLM layers). The MZI and its vicinity presented a lower number of pores and no cracks were observed.
- The tensile strength test showed that the MZI was not the fragile zone of the hybrid specimens. The rupture occurred in the middle of the SLMed portion, around 5 mm from the MZI, although the ultimate tensile strength was ~7% lower than that of the ordinary rolled material. Thus, the hybrid-manufacturing process did not significantly reduce the resistance of the hybrid specimens.
- Considering the SLM process as the second constraint of the hybrid process, it was observed that as the distance from the MZI increases, the number of pores increases slightly. However, the density of the SLM portion of the specimens was around 99.7%, which is expected in an ordinary SLM process.
- There is a tendency for the hardness to reduce in this region of the SLM portion (5 mm from the melting zone interface), but the hardness reduced by only around 2% (346 ± 6 HV0.5) and it was very similar to that of the substrate.
- The hybrid-manufacturing process was found to be a suitable alternative to reduce manufacturing costs and time. With the use of the mold manufactured in this study, this process saved around 53% in terms of costs and reduced the SLM manufacturing time by around 60%.
- The injection molding process reaches the steady-state regime within the first few cycles with the proposed conformal cooling channels, which is not the case with the baffle mold. This reduces the wastage of material.
- The temperature measured on the proposed conformal cooling mold was ~60% lower than that of the mold with baffle inserts, at the end of one molding cycle. Simulations showed a high homogeneity of the temperature on the conformal cooling inserts. To obtain similar homogeneity using the baffle insert, the injection molding time needs to be extended by 36%.
- The mold with conformal cooling resulted in plastic parts without internal defects. This is because the temperature homogeneity increased by a factor of 10, reducing the dimensional error by a factor of 7.

In general, the hybrid-manufacturing process is reliable, and provides an attractive alternative, saving manufacturing

costs and time. The proposed bifurcated conformal cooling design produces better plastic parts and reduces the injection time. Therefore, the results reported herein demonstrate the potential of the concept investigated and suggested topics for future work include investigating the following:

- The influences of the SLM process parameters on the MZI in hybrid manufacturing.
- Mechanical and thermal fatigue in parts manufactured by the hybrid process.
- The precision of the CAE simulation for bifurcated conformal cooling design.

Acknowledgements Development agencies and institutions: Coordination of Superior Level Staff Improvement (CAPES), National Council for Scientific and Technological Development (CNPq). Partners and industries: BMW-Brazil, CFAA, GPCAM, Polimold, Sandvik Coromant, SIGMASOFT, Sokit Ind., Techcontrol, Tecnodrill, Tecnomotriz, Villares Metals, and Vtech.

Author contribution Felipe Marin: manufactured the samples (SLM and machining) and the mold for injection molding of plastic parts. Performed injection molding process to produce the workpieces and analyses. Drafted the manuscript.

Adriano Fagali de Souza: planned and coordinated the research project and its funding. Analysis and discussion about the results of SLM and the entire manufacturing costs and times. Coordinated the laboratory activities. Written the final version.

Carlos Henrique Ahrens: analysis and discussion about the results of SLM and the plastic parts. Collaborated to write the literature review and the final version.

Luis Norberto López de Lacalle: general supervision of the work. Analysis and discussion about the results about SLM. Contributed with the structuring of the paper and final revision.

Funding This project was supported by grants from the Coordination of Superior Level Staff Improvement (CAPES), UFSC Project/CJ/001-2016 and the National Council for Scientific and Technological Development (CNPq-315232/2018-8).

Availability of data and material (data transparency) The datasets obtained during the current work are available from the corresponding author upon request.

Declarations

Competing interests The authors declare no competing interests.

Disclaimer The authors declare that the paper is original and has been written based on the authors' own finding. All the figures and tables are original, and every expression from other published works was acknowledged and referenced. It is confirmed that all the authors are aware and satisfied of the authorship order and correspondence of the paper.

References

1. Park HS, Dang XP (2010) Optimization of conformal cooling channels with array of baffles for plastic injection mold. *Int J Precis Eng Manuf* 11:879–890. <https://doi.org/10.1007/s12541-010-0107-z>

2. Zheng Z, Zhang H, Wang G, Qian Y (2011) Finite element analysis on the injection molding and productivity of conformal cooling channel. *J Shanghai Jiaotong Univ* 16:231–235. <https://doi.org/10.1007/s12204-011-1128-1>
3. Mohamed OA, Masood SH, Saifullah A (2013) A simulation study of conformal cooling channels in plastic injection molding. *Int J Eng Res* 2:344–348
4. Mazur M, Leary M, McMillan M, Elambasseril J, Brandt M (2016) SLM additive manufacture of H13 tool steel with conformal cooling and structural lattices. *Rapid Prototyp J* 22:504–518. <https://doi.org/10.1108/RPJ-06-2014-0075>
5. Abbès B, Abbès F, Abdessalam H, Urganlar A (2019) Finite element cooling simulations of conformal cooling hybrid injection molding tools manufactured by selective laser melting. *Int J Adv Manuf Technol* 103:2515–2522. <https://doi.org/10.1007/s00170-019-03721-2>
6. Park HS, Dang XP (2017) Development of a smart plastic injection mold with conformal cooling channels. *Procedia Manuf* 10:48–59. <https://doi.org/10.1016/j.promfg.2017.07.020>
7. Liu C, Yan D, Tan J, Mai Z, Cai Z, Dai Y, Jiang M, Wang P, Liu Z, Li CC, Lao C, Chen Z (2020) Development and experimental validation of a hybrid selective laser melting and CNC milling system. *Addit Manuf* 8604:101550. <https://doi.org/10.1016/j.addma.2020.101550>
8. Marin F, Miranda JR, Souza AF (2018) Study of the design of cooling channels for polymers injection molds. *Polym Eng Sci* 58:552–559. <https://doi.org/10.1002/pen.24769>
9. Dang XP, Park HS (2011) Design of u-shape milled groove conformal cooling channels for plastic injection mold. *Int J Precis Eng Manuf* 12:73–84. <https://doi.org/10.1007/s12541-011-0009-8>
10. Mayer S (2009) Optimised mould temperature control procedure using DMLS. *EOS e-Manufacturing Sol.* 1–11
11. Park HS, Pham NH (2009) Design of conformal cooling channels for an automotive part. *Int J Automot Technol* 10:87–93. <https://doi.org/10.1007/s12239-009-0011-7>
12. Marques S, Souza AF De, Miranda J, Yadroitso I (2015) Design of conformal cooling for plastic injection moulding by heat transfer simulation. 25:564–574. <https://doi.org/10.1590/0104-1428.2047>
13. Wang Y, Yu K-M, Wang CCL, Zhang Y (2011) Automatic design of conformal cooling circuits for rapid tooling. *Comput Des* 43:1001–1010. <https://doi.org/10.1016/j.cad.2011.04.011>
14. Xu X, Sachs E, Allen S (2001) The design of conformal cooling channels in injection molding tooling. *Polym Eng Sci* 41:1265–1279. <https://doi.org/10.1002/pen.10827>
15. Weidenfeller B, Höfer M, Schilling FR (2004) Thermal conductivity, thermal diffusivity, and specific heat capacity of particle filled polypropylene. *Compos Part A Appl Sci Manuf* 35:423–429. <https://doi.org/10.1016/j.compositesa.2003.11.005>
16. Kennedy P (1999) CAD, CAM, & CAE. Lexingt. Mould, Corp
17. Li CS, Shen YK (1995) Optimum design of runner system balancing in injection molding. *Int Commun Heat Mass Transf* 22:179–188. [https://doi.org/10.1016/0735-1933\(95\)00003-8](https://doi.org/10.1016/0735-1933(95)00003-8)
18. Clemente MR, Panão MRO (2018) Introducing flow architecture in the design and optimization of mold inserts cooling systems. *Int J Therm Sci* 127:288–293. <https://doi.org/10.1016/j.ijthermalsci.2018.01.035>
19. Rahim SZA, Sharif S, Zain AM, Nasir SM, Mohd Saad R (2016) Improving the quality and productivity of molded parts with a new design of conformal cooling channels for the injection molding process. *Adv Polym Technol* 35:35. <https://doi.org/10.1002/adv.21524>
20. Mazur M, Brincat P, Leary M, Brandt M (2017) Numerical and experimental evaluation of a conformally cooled H13 steel injection mould manufactured with selective laser melting. *Int J Adv Manuf Technol* 93:881–900. <https://doi.org/10.1007/s00170-017-0426-7>
21. Ahn DG (2011) Applications of laser assisted metal rapid tooling process to manufacture of molding & forming tools-state of the art. *Int J Precis Eng Manuf* 12:925–938. <https://doi.org/10.1007/s12541-011-0125-5>
22. Souza AF, Al-Rubaie KS, Marques S et al (2019) Effect of laser speed, layer thickness, and part position on the mechanical properties of maraging 300 parts manufactured by selective laser melting. *Mater Sci Eng A* 767:138425. <https://doi.org/10.1016/j.msea.2019.138425>
23. Arrizubieta JI, Cortina M, Mendioroz A et al (2020) Thermal diffusivity measurement of laser-deposited AISI H13 tool steel and impact on cooling performance of hot stamping tools. *Metals (Basel)* 10. <https://doi.org/10.3390/met10010154>
24. Arrizubieta JI, Lamikiz A, Cortina M, Ukar E, Alberdi A (2018) Hardness, grain size and porosity formation prediction on the Laser Metal Deposition of AISI 304 stainless steel. *Int J Mach Tools Manuf* 135:53–64. <https://doi.org/10.1016/j.ijmactools.2018.08.004>
25. Fergani O, Berto F, Welo T, Liang SY (2017) Analytical modelling of residual stress in additive manufacturing. *Fatigue Fract Eng Mater Struct* 40:971–978. <https://doi.org/10.1111/ffe.12560>
26. (2016) Uddeholm Corrax. In: Uddeholm Corrax Tech. datasheet. https://www.uddeholm.com/files/PB_Uddeholm_corrax_english.pdf. Accessed 20 Sep 2020
27. Gong H, Rafi K, Gu H, Starr T, Stucker B (2014) Analysis of defect generation in Ti–6Al–4V parts made using powder bed fusion additive manufacturing processes. *Addit Manuf* 1–4:87–98. <https://doi.org/10.1016/j.addma.2014.08.002>
28. Choi J-P, Shin G-H, Yang S, Yang DY, Lee JS, Brochu M, Yu JH (2017) Densification and microstructural investigation of Inconel 718 parts fabricated by selective laser melting. *Powder Technol* 310:60–66. <https://doi.org/10.1016/j.powtec.2017.01.030>
29. Torres-Alba A, Mercado-Colmenero JM, Diaz-Perete D, Martín-Doñate C (2020) A new conformal cooling design procedure for injection molding based on temperature clusters and multidimensional discrete models

Publisher's note Springer Nature remains neutral with regard to jurisdictional claims in published maps and institutional affiliations.

A new approach to dynamic forecasting of cavity pressure and temperature throughout the injection molding process

Rodolfo Gabriel Pabst¹  | Adriano Fagali de Souza¹ | Alexandro Garro Brito¹ | Carlos Henrique Ahrens²

¹Federal University of Santa Catarina, Dona Francisca, Joinville, Santa Catarina, Brazil

²Federal University of Santa Catarina, Eng. Agrônomo Andrei Cristian Ferreira, Florianópolis, Santa Catarina, Brazil

Correspondence

Rodolfo Gabriel Pabst, Federal University of Santa Catarina, Dona Francisca, n° 8300, Postal Code: 89201-250, Joinville, Santa Catarina, Brazil.

Email: rodolfopabst@hotmail.com

Funding information

Conselho Nacional de Desenvolvimento Científico e Tecnológico (CNPq); Coordenação de Aperfeiçoamento de Pessoal de Nível Superior (CAPES); Fundação de Amparo a Pesquisa e Inovação de Santa Catarina (Fapesc), Grant/Award Number: 2022TR001437

Abstract

The injection molding process is very sensitive to ordinary environmental alterations, as the numerical simulation is limited to within one injection cycle, and it cannot predict transient regimes. The present study presents a new approach based on SARIMAX models developed to predict the temperature and pressure inside the mold cavity. The proposed approach was developed in Python language, and it can identify the behavior of the process, allowing preventive actions. Experimental data of temperature and pressure obtained in real-time inside an injection mold were accessed to use and to validate the proposed model. The results showed its efficiency and its high accuracy for predicting variations in temperature and pressure inside the mold, even when using a small number of samples to be trained. The proposed model can be very useful for monitoring the production of mechanical parts, under an Industry 4.0 environment. For future works, the model enables a contribution toward digital twins of a molded part, considering all the alteration on the parts' properties due to the disturbance on the injection molding process. Furthermore, it lays the groundwork for a new injection machine control system architecture.

KEYWORDS

injection molding, modeling, monitoring, pressure and temperature

1 | INTRODUCTION

Today, the injection molding process is the most used method for manufacturing plastic parts in large scale and has grown rapidly in the past three decades, replacing metal parts with plastic ones in different industrial sectors such as the automotive, electronic, and medical.^[1] The process mainly comprises the following stages: filling, packing, holding, and cooling. After the filling stage, the cavity pressure shows a rapid growth (packing stage) and a switchover changes the process control from a flow-based control to a pressure-based control. In the holding stage, more material is injected until the

injection point (the gate) freezes to compensate the thermal contraction.

The quality of the molded part, in terms of geometric accuracy, sink marks, and mechanical properties are strongly influenced by the parameters set along the injection cycle such as the molten polymer temperature, reciprocating screw advance velocity, and holding pressure. These parameters are defined by the user, but the properties of the molded part are also affected by the mold geometry and by transfer phenomena within the cavity mold.

The process dynamics together with the complex cavity geometries make injection molding a sensitive

process, and any simple alteration can affect the quality of the manufactured parts. According to Sadeghi,^[2] variance in melt flow index (MFR) is one of the major causes of variation in part properties. Among the different sources of disturbances, Yang and Gao^[3] attribute the main effects to: temperature sensitive characteristics in polymer, hydraulic oil, and machine components; and nonlinearities in servo valves behavior.

Today, numerical simulations by computer-aided engineering software (CAE) are the most used tool to simulate this injection molding process. The investigation presented by Marin et al.^[4] demonstrated that current CAE software can achieve high accuracy for predicting temperature and pressure inside mold cavities during injection processes (98% and 97%, respectively), but it takes into account the process dynamics only within one injection cycle. Thus, transient regimes due to thermal perturbations or variations in the polymer properties cannot be predicted by CAE approaches.

Therefore, the present study addresses this issue and presents a statistical model to forecast injection cycles ahead of a batch production of plastic parts. By using a SARIMAX framework the cavity temperature and pressure profiles were modeled as mixed autoregressive moving average processes. The proposed model is able to forecast the variations that usually occur cycle-to-cycle in an injection molding batch, which the CAE cannot predict. The method was validated to profiles obtained from a real process and to profiles with simulated deterministic disturbances. The fulfillment of real time requirements show that it is possible to employ this method on simple open-loop control approaches. Furthermore, the method lays the groundwork for a new closed-loop control for the injection molding process.

2 | LITERATURE REVIEW

To support the development of this study, a literature review on the injection molding process and forecasting was carried out and is presented below.

2.1 | Injection molding variables and data acquisition

The process data can be classified by means of process variables and machine variables. The process variables refer to the data that occur inside the mold cavity during an injection cycle. The pressure-volume-temperature (PVT) data and the flow velocities are the main process variables. Hydraulic pressures, clamping forces, and reciprocating screw strokes or velocities are known as

machine variables. Some studies have been conducted to improve the process variables measurements because these variables more adequately represent the injection process and the quality of the molded products.^[5,6] This is due to the dependence of the mass and heat transfer during injection molding in relation to the cavity geometry.

Some results of the molded part, such as weight, morphology, sink marks, and shrinkage and warpage are largely defined by the cavity pressure. This correlation between the cavity pressure and the part quality makes the cavity pressure a major issue in the monitoring and control of the process.^[7]

The cavity pressure is relevant, especially, in the filling and packing-holding stages. After the gate is frozen, a stage with constant volume begins. This isochoric stage is important for the dimensional accuracy of the molding. The setting of the cavity temperature, at the end point of the holding stage, can be used to adjust the cooling time to produce parts with optimum qualities.^[8]

Chen and Gao^[9] studied the influence of the packing-holding pressure profile on the part quality. They concluded that the part weight is a non-monotone function of the packing-holding pressure. Phenomenon like part warpage or part shrinkage are profile dependent.

Nam et al.^[10] used cavity pressure and temperature signals to model the form error in injection molded lenses through a response surface methodology (RSM). The comparison with experimental results showed that PVT data inside mold cavity can be used to predict the quality of the injected parts. Wang and Mao^[11] show that the PVT data can also be used in the injection mold process control. Marin et al.^[12] showed that the form error in molded plastic parts is strongly influenced by the temperature inside the mold's cavity, and it can also cause voids inside the plastic parts.

Considering this background, the monitoring of the process inside the mold's cavity is justified. Although control approaches by means of machine variables have shown good results, they guarantee only the cycle-to-cycle reproducibility of machine variables. Since the quality of the injected parts are dependent on mold geometry, the control and monitoring of process variables are a major issue for the injection molding process.

2.2 | Modeling approaches for injection molding processes

Currently, three main modeling approaches of the transfer phenomena within injection molding processes can be found in the literature. These approaches comprise analytical and numerical solutions to differential partial

TABLE 1 Comparison between modeling approaches

| | Analytical models | CAE simulations | Empirical models |
|------------|---|---|--|
| Geometry | Simple geometric shapes (cylindrical pipes and parallel planes) | Complex geometries approximated by polygonal meshes | Geometry is not necessary. Data obtained by sensor along the process |
| Parameters | Diffusivity parameters and thermodynamic state | Diffusivity parameters and thermodynamic state | Parameters estimated through process data |
| Dynamics | Within stage behaviors | Within cycle behaviors | Within cycle and seasonal behaviors |

equations based on processes with physical or empirical models based on process data.

Analytical models can be obtained by solving mass, momentum, and energy conservative equations whose initial and boundary values represent the process conditions. Solutions to steady state incompressible flows can be found in works by Bretas and D'ávila,^[13] while pulsatile incompressible flows were investigated by Daprà and Scarpi.^[14] The temperature evolution on a slab of polymer within the mold cavity is the subject of a study by Pignon et al.^[15] However, this procedure is limited to very restricted conditions in simple geometries, and it can represent only dynamic behaviors within the stages of the injection cycle.

Usually, CAE software simulates the injection molding process by employing the Hele–Shaw model, which is based in a simplification of the conservation equation of momentum considering the flow laminar, incompressible and invariant along the part width. Solutions to this model can be approximated on a mesh of polygonal domains through the finite elements method.^[16] However, it is a time varying process and the part's properties can suffer unpredictable alterations along a production batch.^[3] Since these disturbances can be stochastic, the CAE simulation cannot take them into account. Thus, it is limited to simulate the process dynamic within one injection cycle, neglecting seasonal disturbances.

Empirical models are able to address these seasonal disturbances. Unlike analytical models and CAE simulations, empirical models do not require total knowledge of the mold cavity's geometry. It requires data from the process, obtained by transducers or from the machine's CLP. The knowledge of material parameters is not needed as well, since the model parameters can be estimated by statistical procedures.

Table 1 provides an overview of these different modeling approaches to modeling the injection molding processes and its particularities. Each method has specific properties, considering the geometry, parameters, and dynamics.

Depending on the purpose, one method may be more suitable than another to represent the process.

Considering the complex geometry and the seasonal disturbances usually faced in injection molding processes, as well as the intention to develop a model for a future closed looping control, the present study focuses on empirical models.

2.3 | Empirical modeling for injection molding process

To contextualize the state-of-art of modeling for the injection molding process, a chronological background is presented below.

One of the first models to forecast the injection molding process was presented by Haber and Kamal.^[17] The authors used the Box and Jenkins method to model the peak values of the cavity pressure in an injection molding process. The model was able to identify a second order autoregressive behavior on the peak pressure time series. However, the modeling did not comprise the entire cavity pressure profile.

Contemporarily, Kamal et al.^[5] developed a deterministic model of the cavity pressure dynamics during the filling stage of an injection molding cycle. In order to generate data to fit the model parameters, the authors performed steps on the servovalve, which controls the reciprocating screw stroke. The model consisted of a first order plus delay response superimposed to a constantly increasing pressure. The model is represented by the Equation 1:

$$p(t) = K_1 t + K_2 \left(1 - e^{-\frac{t-D}{\tau}}\right), \quad (1)$$

where $p(t)$ is the cavity pressure, K_1 and K_2 are constant parameters, D is a time delay, and τ is a constant of time. The delay was attributed to the distance between the gate and the location of the pressure transducer. This work represented a step forward, but again, the model cannot forecast the entire profile of the pressure during a molding cycle, which limits the forecasting of the process.

Kamal et al.^[5] also tried to fit a stochastic model by performing steps on the servovalve according to a pseudorandom binary sequence (PRBS). The Box and Jenkins method was used to obtain a transfer function relating the servovalve opening to the cavity pressure. However, the stochastic model had not successfully represented the differenced pressure time series. The authors attributed this to excessive noise in the measurements.

Zhao and Gao^[18] developed a model to obtain a profile correlating the nozzle temperature to the reciprocating screw stroke. In this profile, the initial and final temperature (and its extreme values as well) and their respective strokes were selected. These points were used as an artificial neural network (ANN),^[19] while the injection stroke and another process settings were used as the inputs. The ANN was trained with 25 sets of experimental data through 10,000 epochs reaching a global error goal of 0.1%. After this, the temperature profile was reconstructed using a piece-spline method based on the ANN outputs. Although the good accuracy shown in the results, this model does not comprise the dynamics of the process, since the nozzle temperature is related to the reciprocating screw stroke instead of its previous values or time derivatives.

Sadeghi^[2] developed an off-line planning process utilizing an artificial neural network (ANN) and the results of CAE simulation of the molding process using a high-density polyethylene (HDPE). The results were used to train an ANN capable of predicting short shot and weld line defects. The ANN was trained with the results of 2000 simulations through 660 epochs using a backpropagation algorithm. The occurrence of short shot and weld line defect phenomenon could be predicted by the ANN for process parameters settings absent in the simulations. This demonstrated a good generalization capacity of the ANN. It is possible to point out that the approach proposed by Sadeghi^[2] required much less computational time than the approach by Zhao and Gao.^[18] This happened due to the size of the data set used to train the model, implying that a huge data set is needed when the time to fit the model plays a critical role. But again, the procedure did not take into account the process dynamics.

Following the development sequence, Zhao et al.^[20] used an ANN to forecast the cavity pressure. For this aim, an ultrasonic transducer generated pulsed ultrasounds inside the cavity and received the reflected response at the cavity interface. To indicate the material density inside the cavity, a reflection coefficient was calculated through the ratio between the incident and the reflected ultrasounds amplitudes. Thus, the reflection coefficient, the cavity temperature, and the hydraulic pressure were used as inputs of an ANN. The cavity

pressure (measured with a Kistler 6190A sensor) was used as the output. The forecasts provided by the ANN presented good agreement with the experimental data (the maximum error was less than 0.6 MPa). This work represented a great advancement in this field, but it is a static model. Thus, it is limited to being implemented in a forecast or in a control approach. ANN require an amount of training data, which may not be conveniently identified in real time process.^[2] SARIMAX models can be an important alternative to predict time series with periodic behavior, as in the case of injection molding.^[21]

Another ultrasonic method to measure the cavity pressure was proposed by Zhang et al.^[22] The method is based on the tensile elongation of the machine's tie bar due to the cavity pressure and clamping force. According to sonoelasticity theory, the stress on the tie bar is proportional to the time interval required for a pulsed ultrasound to be reflected at the tie bar ends. To calibrate this method, the cavity pressure was measured with a Kistler 6157B sensor. Despite of the good agreement with experimental data (4.3% of relative error), this method requires the use of appropriate clamping force profiles to produce accurate forecasts.

The literature review showed that there is a lack of modeling approaches to cavity temperature and pressure in injection molding processes, considering these variables dynamics. In order to obtain an efficient forecasting for monitoring and controlling the process, it is necessary to generate a model of the process dynamics that comprises cycle-to-cycle variations.

The present work introduces a new real-time statistical approach to predict the variable profile during a batch of production of molding parts. Temperature and cavity pressure were considered as the process variables. The proposed model can provide reasonable one-cycle prediction for process behavior. This can be useful to monitor the characteristics of the next molding part to be produced. Furthermore, the methodology can also be used to actively actuate into the process to prevent failures in the next parts.

3 | MODELING FRAMEWORK

SARIMAX models were used to model the process variables. SARIMAX models are statistical methods used to identify processes such as time series. They do this by adjusting the coefficients, and can be used to understand the behavior of the time series and forecast future values. This kind of model is a generalization of the mixed autoregressive moving average (ARMA) processes. ARMA models cannot identify nonstationary behaviors in the time series, while SARIMAX does this by differentiating

the signals.^[21] Due to the seasonality in cavity pressure and temperature, SARIMAX was evaluated in this study.

SARIMAX models can represent more parsimoniously the injection molding process. This is because these models can frame periodic behaviors through differentiating the signals. The differentiated signals, in turn, can be identified as a mixed linear autoregressive moving average process, since the cycle-to-cycle deviations are small.

After performing preliminary tests with the models, it was observed that using the cavity temperature and the cavity pressure as covariables resulted in a significant reduction of the mean squared error for the forecasts of the process variables. Therefore, SARIMAX models were implemented by including the covariables as exogenous variables.

The basis used to develop the model proposed in the work involves the following methods: ARMA, ARIMA, SARIMA, and SARIMAX. A description of each method and its correlation with the developed model is presented ahead.

3.1 | ARMA and ARIMA models

Prior to a deeper description on the proposed SARIMAX modeling for the injection molding process, some notation and general concepts should be posed. Let be a continuous experimental data $y(t)$, properly sampled with a sample time T_s , resulting in a discrete-time data $[y_1 \ y_2 \ \dots \ y_k \ \dots]$ where y_i denotes the i th sample value of such data. Define the time-delay operator z^{-l} as

$$z^{-l}y_i \triangleq y_{i-l}, \quad (2)$$

that is, y_{i-l} is the sample data l steps behind the sample y_i . Additionally, consider the functions

$$\begin{aligned} \phi_p &\triangleq \phi(z^{-1}, p) = 1 - a_1z^{-1} - a_2z^{-2} - \dots - a_pz^{-p} \\ \theta_q &\triangleq \theta(z^{-1}, q) = 1 - b_1z^{-1} - b_2z^{-2} - \dots - b_qz^{-q} \end{aligned} \quad (3)$$

as discrete polynomials in time-delay operator.

The AutoRegressive AR model of order p refers to the data description of the variable in terms of its past values, that is,

$$y_t = a_1y_{t-1} + a_2y_{t-2} + \dots + a_py_{t-p} + \epsilon_t \Rightarrow \phi_p y_t = \epsilon_t, \quad (4)$$

where ϵ_t is the modeling error, which includes noise and non-modeled dynamics.

The Moving Average MA model of order q takes into account the stochastic contributions in the formation of the present value of the modeled variable. By assuming ϵ_t a white noise, whose ϵ_t and ϵ_{t-l} are uncorrelated for any $t \neq 0$ and $l \in \mathbb{Z}$, the MA model is given by

$$y_t = b_0\epsilon_t + b_1\epsilon_{t-1} + b_2\epsilon_{t-2} + \dots + b_q\epsilon_{t-q} \Rightarrow y_t = \theta_q\epsilon_t. \quad (5)$$

The ARMA model of order (p, q) is obtained by considering the two contributions above, that is, $\phi_p y_t = \theta_q \epsilon_t$.

A stochastic process is referred as *nonstationary* if its statistic characteristics, measured by the sample average and variance, are not constant along the time. A known result on regressive modeling is that an ARMA model is not suitable to describe nonstationary data.^[21] When the data presents a nonstationary character, it is necessary to include an additional Integrated term, of order d , into the model. This term consists in differentiating the experimental data by d steps, so that the processed data results in a stationary condition. For instance, the operation $(1 - z^{-1})y_t = y_t - y_{t-1}$ produces a data which two consecutive values are subtracted themselves. Then, this can be extended to a general order of differentiating d , resulting in the ARIMA model of order (p, d, q) :

$$\phi_p(1 - z^{-1})^d y_t = \theta_q \epsilon_t. \quad (6)$$

3.2 | SARIMA and SARIMAX models

A Seasonal AutoRegressive Integrated Moving Average—SARIMA—model is the one that blends the ARIMA model features and the previous knowledge about seasonality in the data profile. If the data presents a season period s , one can obtain a SARIMA model by using the general formulation^[21]:

$$\phi_p z^{-s} \Phi_P (1 - z^{-1})^d (1 - z^{-s})^D y_t = \theta_0 + \theta_q z^{-s} \Theta_Q \epsilon_t, \quad (7)$$

where ϕ_p , Φ_P , θ_q and Θ_Q are functions with their own parameters and order and θ_0 is a constant parameter. When this parameter is zero, the model can only describe stochastic processes. Otherwise, deterministic behaviors can be represented. The model can be expressed by the compact format $SARIMA(p, d, q) \times (P, D, Q)_s$, in which $(P, D, Q)_s$ represents, respectively, the regressive, integrated and moving average orders for the seasonality description, while (p, d, q) are the orders of the ARIMA contribution.

Notice that all the models discussed until this point explains the experimental data by a regression of past values of such variable, its season character and moving average aspects. However, some process variables can be correlated to another, what implies that a richer model is only achieved if this additional variable is also included into the model. For example, it is expected that the temperature profile exerts influence over the cavity pressure variable and vice-versa. Hence, this called exogenous variable can be introduced into the SARIMA model, resulting in the Seasonal AutoRegressive Integrated Moving Average with eXogenous inputs—SARIMAX—models.

From the mathematical point of view, a SARIMAX model can be described as follows. Let y_t be the process variable to be explained, and x_t another process variable. Consider the function

$$\gamma_r \equiv \gamma(z^{-1}, r) = 1 + c_1 z^{-1} + c_2 z^{-2} + \dots + c_r z^{-r}. \quad (8)$$

Then, a SARIMAX(p, d, q) \times (P, D, Q) $_s$ model for the variable y_t that takes into account the effects of the exogenous input x_t is written as

$$\phi_p z^{-s} \Phi_P (1 - z^{-1})^d (1 - z^{-s})^D y_t = \theta_0 + \theta_q z^{-s} \Theta_Q \epsilon_t + \gamma_r x_t. \quad (9)$$

One of the main features of the SARIMAX models is their ability to forecast future experimental values of a dynamic process. This is useful not only for control purpose, but also for process quality assurance.

For one-cycle ahead forecasting, it might be considered that all data were measured until the time t , and the model should provide forecasting for the variable values between the time interval $t+1$ and $t+s$, where s represents the season periodicity. These forecast values are denoted herein as $\hat{y}_{t+1:t+s}$. However, to obtain such values in a SARIMAX framework, some information should be available at the forecast moment t :

- Previous values for the process variable $y_{0:t}$ and exogenous input $x_{0:t}$, which is not a problem, since the experimental data is acquired in real-time;
- Forecast values for the exogenous input $\hat{x}_{t+1:t+s}$.

By assuming that the exogenous input has also a seasonal profile, a strategy should be applied to obtain $\hat{x}_{t+1:t+s}$ prior the estimation of a one-cycle ahead ($\hat{y}_{t+1:t+s}$) through the SARIMAX model. This paper proposes a methodology to obtain such input forecast in Section 4.3.

4 | EXPERIMENTAL PROCEDURE

The developed model was tested in a real injection molding process. The validations were conducted in two situations: (i) changing the process filling time (three values) and (ii) under deterministic disturbances that can occur during any batch of parts manufactured by injection molding process.

Based on SARIMAX approach, an empirical model was developed using Python language and the process variables, that is, cavity temperature and pressure. Thereby, the proposed system predicts the process variables' behavior in seasonal intervals based on temperature and pressure samples obtained in real-time by transducers installed inside the mold cavity, such as thermocouples and piezoelectric sensors, respectively.

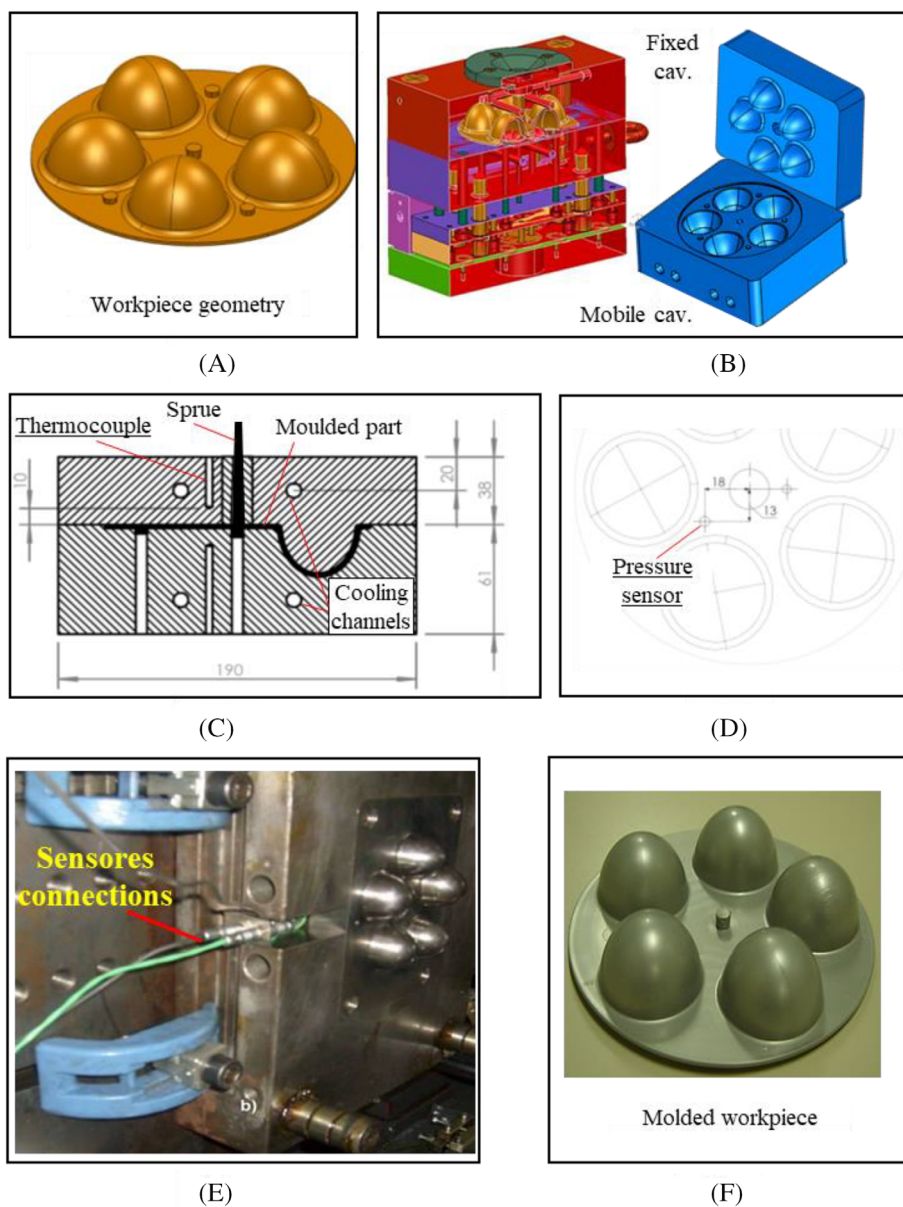
The model was designed in two stages. First, one should obtain a SARIMAX structure for the process. This model structure is based on the parameters p, q, r and P, Q, R of the SARIMAX model, and the seasonal time s (Equation 9). This structure is often related to the process operational conditions, such as filling time and part to mold. One way to obtain the model structure is performing a previous test with a variety of conditions for the parameters p, q, r and P, Q, R . The chosen structure is the one that minimizes some design metrics. Once the model structure is defined, the second stage consists in obtaining the model coefficients of the polynomials ϕ_p, Φ_P, θ_q , and Θ_Q . Therefore, it means that for each mold (product) and process parameters, a new model and its parameters might be developed. Both design stages are presented in the current work.

The experimental procedure is divided into: (i) workpiece, mold, data acquisition and validation of the proposed model; (ii) preliminary data processing; (iii) design of the SARIMAX model and its parameters; (iv) results and discussions, as detailed in the following sections.

4.1 | Workpiece, mold, data acquisition, and validation of the proposed model

For this work, a product containing free-form shape was designed as a representative workpiece (Figure 1A) as well as its corresponding injection mold (Figure 1B). Sensors of temperature and pressure were installed inside the mold's cavity (Figure 1C,D, respectively). The K-type thermocouples and a Kistler 6190CA piezoelectric sensor were used to measure the cavity temperature and pressure. A Kistler 5139A221 charge amplifier, connected to an Agilent 34970 data acquisition device, was utilized to read the voltage signal.

FIGURE 1 Main basis for the experimental procedure



After manufacturing the mold, the sensors were installed (Figure 1E) and a number of batches of the workpiece (Figure 1F) were carried out using a polypropylene (PP) H105. The plastic workpiece was 140 mm in diameter with 2 mm thickness and was injected into the mold cavity by means of a direct injection system of cold runner type. For this, a HAITIAN SA1200/410 injection mold machine with screw diameter of 40 mm, with an injection volume of 214 cm³ and clamp force of 1200 kN was used.

The injection channel had conical geometry, with extremity diameters of 6.5 (close to the part) and 4.0 mm, with a total measure of 82 mm. The mold also had a cooling system with two U shaped channels of 8 mm in diameter located at 18 mm from the mold surface. Figure 1C shows the thermocouples at 10 mm from the cavity

surface, and Figure 1D shows the pressure sensor was installed at 22 mm from the injection point.

4.1.1 | Validation of the model

First, to certify the efficiency of the model the filling time process parameter was chosen among three values: 0.5, 1, and 2 s. The pressure and temperature of all cases were assessed during the injection molding process, in real time, to feed the model. The second validation was conducted by using the pressure and temperature data with deterministic disturbances along the molding production (for the process with 1 s of filling time).

Figure 2 presents the real profiles of the temperature and pressure obtained by the sensors, for the process with

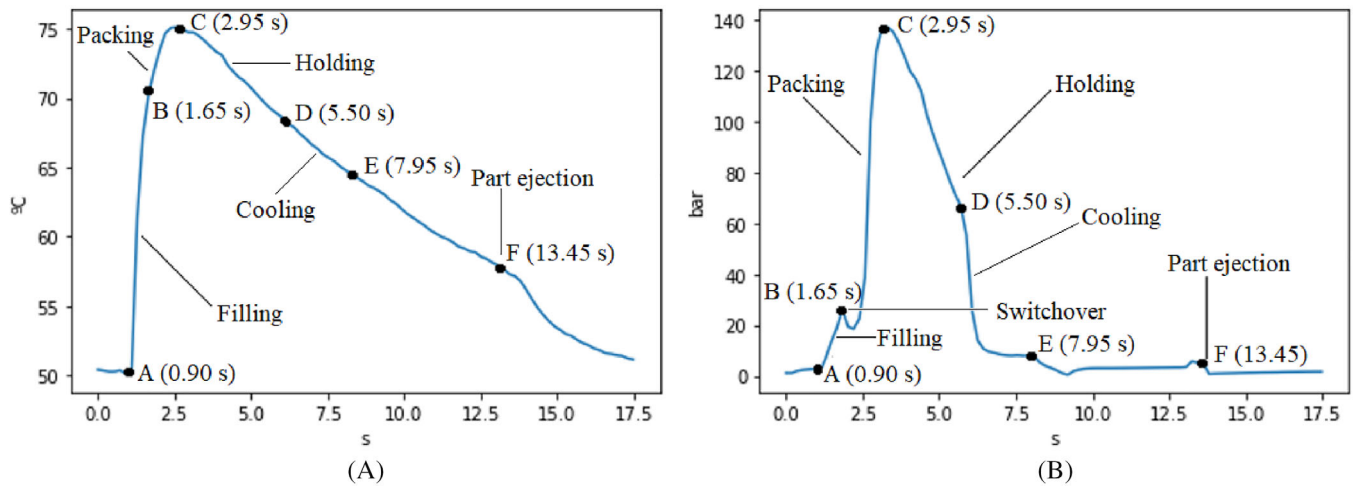


FIGURE 2 Cavity temperature and pressure within an injection cycle: (A) cavity temperature; and (B) cavity pressure

1 s of filling time. These data were feed the model to forecast the future cycles. The points from A to F in Figure 2B delimit the transitions between the injection molding stages. Although the process begins before point A, the molten polymer reaches the pressure sensor location only at this instant. So, the filling stage is comprised between point A and point B, when a switchover from flow-based to pressure-based control occurs.

In Figure 2B, it is possible to see a local minimum between the points B and C. This happens when the switchover occurs before completing the filling of the mold cavity. As a consequence, the compression of the material in the mold cavity starts later under packing-holding pressure. This condition may affect the part quality by inducing deficient weight and poor mechanical characteristics.^[23] In the processes addressed in this work, these local minima were observed for the filling times of 1.0 and 2.0 s, and not for 0.5 s, as presented ahead on the results (Figure 8B). After that, cavity pressure exhibits rapid growth until reaching point C. According to Wang,^[8] during the holding stage a pressure variable is maintained at a predetermined profile while more material is packed into the cavity to compensate thermal shrinkage. Usually, this pressure variable is a machine variable. At point D, the gate freezes, marking the end of the holding stage.

The details about the modeling approaches developed to identify such time series process variables are presented ahead.

4.2 | Preliminary data processing

Because the SARIMAX models require linearity and stationarity for the respective data profile, and the profiles

for the cavity pressure and temperature are nonstationary ones,^[24] the first step of the proposed approach comprises the preprocessing the variables (temperature and pressure) collected in real time during the batch production. Then the prior data processing comprises three steps:

(i) *Outliers removal*: basically, an outlier is defined as a data sample that is considerably discrepant from the expected data profile. This can occur because of some measurement problem at the moment of such point acquisition. There are some methods to detect and treat outliers within experimental data.^[21] In this paper, a statistic approach is applied, as follows. A data sample from the variable process is assumed to be an outlier if its value is outside the range limited by four standard deviations around the data mean. This is an effective method for outlier detection through a statistic z-score test. Once a sample is identified as an outlier, this point is replaced by the mean between the previous and the next samples around it;

(ii) *Nonstationary component removal*: the nonstationary component is removed by taking a differentiated version of the experimental data. By considering the cavity pressure $p(t)$ for instance, the autoregressive model is obtained from the differentiated data $\nabla_{\delta} p_t$ given by

$$\nabla_{\delta} p_t \triangleq p_t - p_{t-\delta}, \forall t, \quad (10)$$

where δ corresponds to the differentiating step delay. Obviously, the strategy can be repeated for another step delay λ :

$$\nabla_{\lambda} \nabla_{\delta} p_t = \nabla_{\lambda} p_t - \nabla_{\lambda} p_{t-\delta}, \forall t. \quad (11)$$

The number of differentiating iterations and the respective step delays should be chosen so that the

stationary condition is achieved. For the injection molding process, a natural choice for the step delay is the season period s , since this is the main contribution for the data nonstationarity. However, a second differentiating iteration can be applied in the case the previous processed data remains nonstationary. The autocorrelation function can be used to test the stationarity of an experimental data (or its differentiated version). For a stationary signal, the autocorrelation function results in a nonnegative even function. Then, the occurrence of significant negative values for the autocorrelation function implies in nonstationarity,^[25] and;

(iii) *Reduction of an eventual nonlinear character*: this is important because the nonlinearity, indeed degrading the data stationarity, also affects the efficacy of the SARIMAX model, once this model is essentially linear. In the present study, the chosen method was the one-parameter Box-Cox transformation, which the data to be modeled pass by a logarithmic function.^[26] For the case of the cavity pressure data, such transformation is relevant, due to its nonlinear profile and its wide value range along the molding process.

4.3 | Design of the SARIMAX model and its parameters

Since the injection molding process can exhibit seasonal order behaviors, as the process variables can also present a nonstationary character, the use of SARIMAX models appears as an attractive option to describe the system. Once the experimental data from the cavity pressure and the temperature were properly preprocessed (Section 4.2), dynamic forecasts of the cavity pressure and temperature were performed.

The statsmodels module, in Python language, allows the dynamic forecasting, also known as n -step ahead prediction. It produces an arbitrary number of predictions by updating the time series with obtained forecasts. The SARIMAX one-cycle ahead forecast depends on future (and not available) values for the process variables. An alternative to circumvent such problem is to model the forecasts within the time $t + 1:t + s - 1$ for each process variable through a SARIMA model, since this provides the variable future values from the own past values for the same variable. These values can then be used with the SARIMAX estimation.

By considering the previous remarks, the proposed SARIMAX s -step ahead forecast methodology can be elaborated according to the following steps:

- Step 1: collect the experimental data from the variables until the present time t ;

- Step 2: obtain the s -step ahead forecast through SARIMA modeling for the process variables. This aims to provide the forecast of the future values $\hat{p}_{t+1:t+s}$ and $\hat{T}_{t+1:t+s}$ to be used in the next step;
- Step 3: obtain the s -step forecast the SARIMAX modeling for the variable process. This is the main step, once the one-cycle ahead prediction takes into account the expected correlation between the process variables;
- Step 4: wait until the next experimental data is available. Then, return to step 1. The procedure can be illustrated by Figure 3.

To verify the forecast performance, standard error measures were used. The mean squared error (MSE), the mean absolute deviation (MAD), and the mean absolute percentage error (MAPE) metrics are defined by:

$$MSE = \frac{1}{T} \sum_{t=1}^T (x_t - \hat{x}_t)^2,$$

$$MAD = \frac{1}{T} \sum_{t=1}^T |x_t - \hat{x}_t|,$$

$$MAPE = \frac{1}{T} \sum_{t=1}^T \frac{|x_t - \hat{x}_t|}{x_t},$$

where \hat{x}_t is the time series forecast in instant t . While MAPE is a measurement, in percent, of prediction accuracy, MAD and MSE are measures of the average magnitude of the forecast errors. However, the latter imposes a greater penalty on a larger error than a significant amount of small errors. Thus, while the MSE measurement enables the visualization of the error peak magnitude, the MAD measurement enables the understanding of the entire forecasting error distribution.

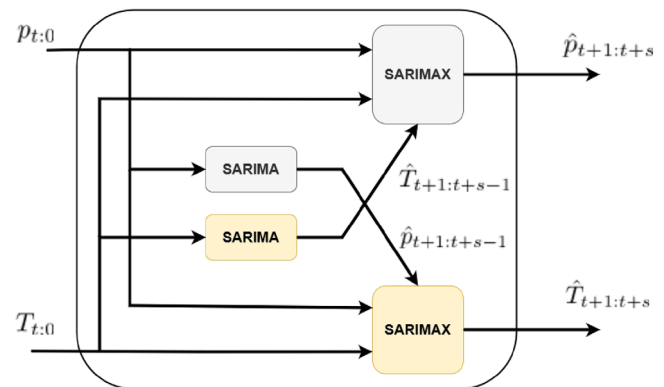


FIGURE 3 SARIMAX framework for the injection process modeling

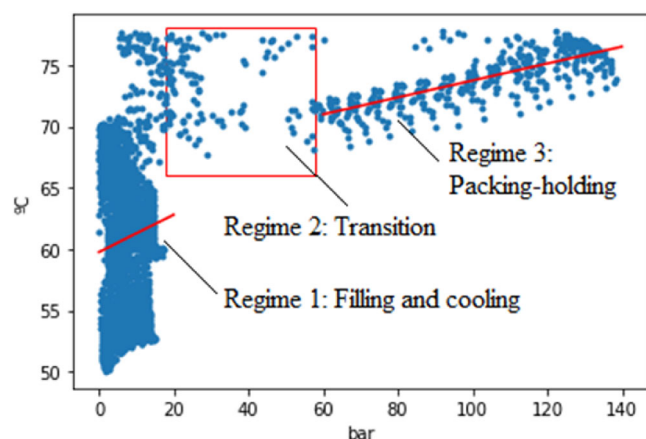


FIGURE 4 Correlation between cavity pressure and temperature

4.3.1 | Correlation analysis in one injection molding cycle

The process variables present correlated behaviors, since they influence each other. To investigate the general aspects concerning the cross-correlation between the process variables, temperature and pressure signals were plotted in a scatter plot, as shown in Figure 4. There are three different regimes along one injection cycle to cite:

- Regime 1: filling and late cooling. In this regime, the points present a huge dispersion, becoming impossible to obtain a linear correlation;
- Regime 2: transition. The region inside the rectangle comprises the early packing and early cooling stages. Once again, a linear correlation is not observed;
- Regime 3: packing-holding. The last regime occurs during the late packing and holding stages, and it presents a linear correlation between cavity pressure and temperature. In Figure 4, the sample data oscillates around the straight line, obtained through the least squares method. The reduction in sample data dispersion can be assigned to the mechanical behavior of the molten polymer during packing-holding stages. According to Zheng et al.^[24] the pressure is a dynamical variable related to the momentum conservation in the flow in incompressible fluids. In compressible fluids it corresponds to the thermodynamic pressure, related to the fluid temperature by an equation of state. This information helps to comprehend the correlation between the process variables and justify their use as covariables during the modeling of the injection molding.

4.3.2 | Evaluation of stochastic and deterministic disturbances

Under ideal conditions, cavity pressure and temperature should present only periodic components. However, it is not rare to occur cycle-to-cycle deviance in the process variables. This can be expressed as mixed autoregressive moving average processes.^[21] An efficient SARIMAX model should be able to express as the steady-state condition as the transient and deviance present into the data.

In order to validate the approach proposed in this work, time series of the process variables, exhibiting significant deterministic transient behaviors, were taken. The Nelder–Mead method was used to identify the process dynamics at each injection cycle. Data samples of five previous cycles were used to forecast the next cycle. Besides the MSE, MAD and MAPE measures, the time required to fit the models was also evaluated.

5 | RESULTS, VALIDATIONS, AND DISCUSSIONS

This section comprises the results of the modeling of the process and the validation of the developed model. Using the real signals of pressure and temperature obtained during several cycles of injection molding to produce the plastic work-piece. The model was evaluated in terms of accuracy. The signals of the first injection cycles were used to fit the model. Later, the signal ahead obtained from the injection process were used to check the accuracy of the forecasted values.

The specific results presented in this section are: (i) preliminary data processing, (ii) design of the SARIMAX model and its parameters; (iii) validation of the model, first under deterministic disturbance that might occur along a production batch and second by applying different molding conditions (different filling time) for the same product.

5.1 | Preliminary data processing

Prior to the modeling task, the experimental data were preprocessed by using the procedure presented in Section 4.2. Indeed important to become possible the SARIMAX modeling, such processing provides valuable information about the injection molding process.

After the stage of outlier removing, the process variables dynamics were evaluated through sample autocorrelation function, as presented in Figure 5. Two facts are remarkable. First, one can observe the periodic aspect due to the data seasonality. The second positive peak, occurring at the lag 96, corresponds to the season period

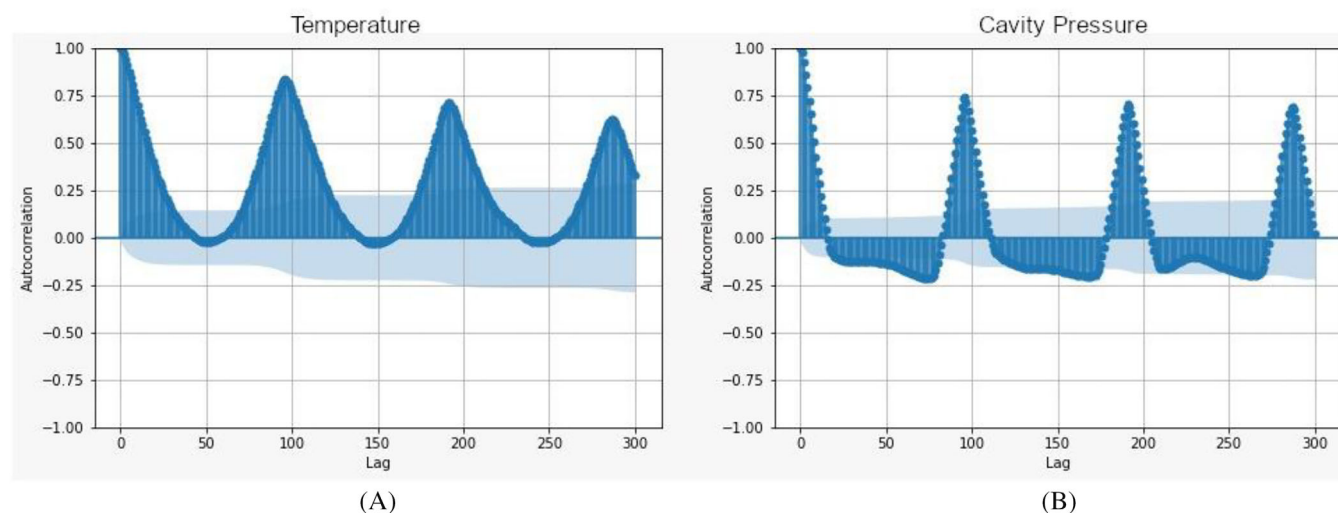


FIGURE 5 Autocorrelation plots for the temperature (A) and cavity pressure (B)

to be further used. Moreover, both data present an obvious nonstationary, and possibly a nonlinear, aspect to be removed prior the modeling stage.

With the information provided above, the time series were first submitted to a seasonal order differentiation (lag $s=96$). The autocorrelation functions can be seen in Figure 6. It is possible to notice that the differentiated temperature time series presents nonnegative autocorrelation, which implies a stationary aspect. However, the pressure time series still presents negative peaks in the autocorrelation plot, even though a seasonal differentiation was applied. This can be explained by a nonlinear aspect in the pressure data.

To circumvent the nonlinearities, the Box–Cox transformation was applied to the data. The results are presented in Figure 7. As expected, the transformation does not considerably impact the temperature data, since this variable already shows an eminent stationary character. However, it resulted in a mostly nonnegative autocorrelation function for the pressure variable (Figure 7B). After this action, the pressured data also presents a stationary aspect, being possible the SARIMAX modeling — a linear methodology.

5.2 | Design of the SARIMAX model and its parameters

In this work, the processed time series of the variables were identified through 108 models obtained by varying the order of the linear operators. The best candidates were chosen by their ability in providing the smallest standard error measures (MSE, MAD and MAPE, for the temperature and MSE and MAD for the pressure) while fitting the model parameters.

The methodology presented in Section 4.3 was applied to obtain the SARIMAX model for the process variables. The next subsections are presented and discussed: (i) the model and its parameters obtained for forecasting the cavity pressure, (ii) the model and its parameters obtained for forecasting the temperature, (iii) the forecasting results using two different optimization algorithms, the BFGS (Broyden–Fletcher–Goldfarb–Shanno) and the Nelder–Mead algorithm.

- i. *The model and its parameters obtained for forecasting the cavity pressure.*

The most suitable parameters are those that result in the minimum values of standard error measures. It happened for SARIMAX $(0, 0, 1) \times (2, 1, 1)_{96}$. Thus, this is the model adopted Equation (12):

$$\begin{aligned} & (1 - \Phi_1 z^{-96} - \Phi_2 z^{-192}) \nabla_{96} P_t \\ & = \theta_0 + \theta_1 T_t + (1 - \theta z^{-1})(1 - \Theta z^{-96}) \varepsilon_t, \end{aligned} \quad (12)$$

where the parameters for the model are: $\Phi_1 = 0.2869$, $\Phi_2 = 0.3103$, $\theta_0 = -0.0119$, $\theta_1 = 0.0852$, $\theta = 0.3185$, and $\Theta = -1.0002$.

- ii. *The model and its parameters obtained for forecasting the cavity temperature.*

Although not necessary from the stationarity point of view, the Box–Cox transformation was also applied to the temperature data. This is because the models presented a slightly better data fitting after such transformation. The minimum error occurred for the SARIMAX $(2, 0, 1) \times (2, 1, 1)_{96}$. Thus, this is the model adopted:

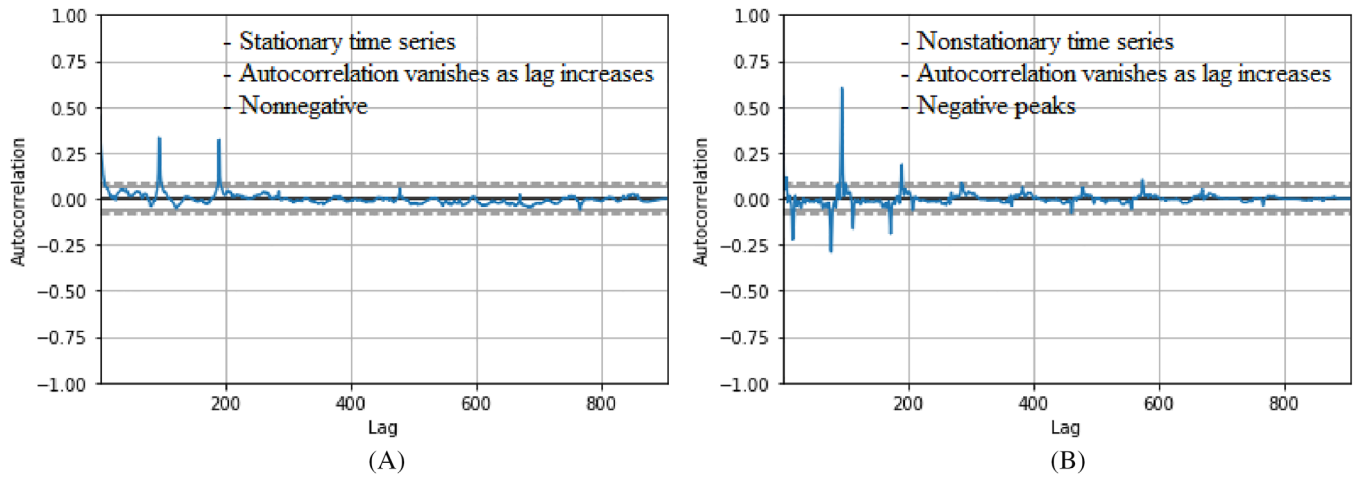


FIGURE 6 Seasonal order differentiation. Differenced temperature (A) and differenced pressure (B) autocorrelation functions. The gray lines represents the confidence levels for the autocorrelation test. The textual information presents the main plot findings

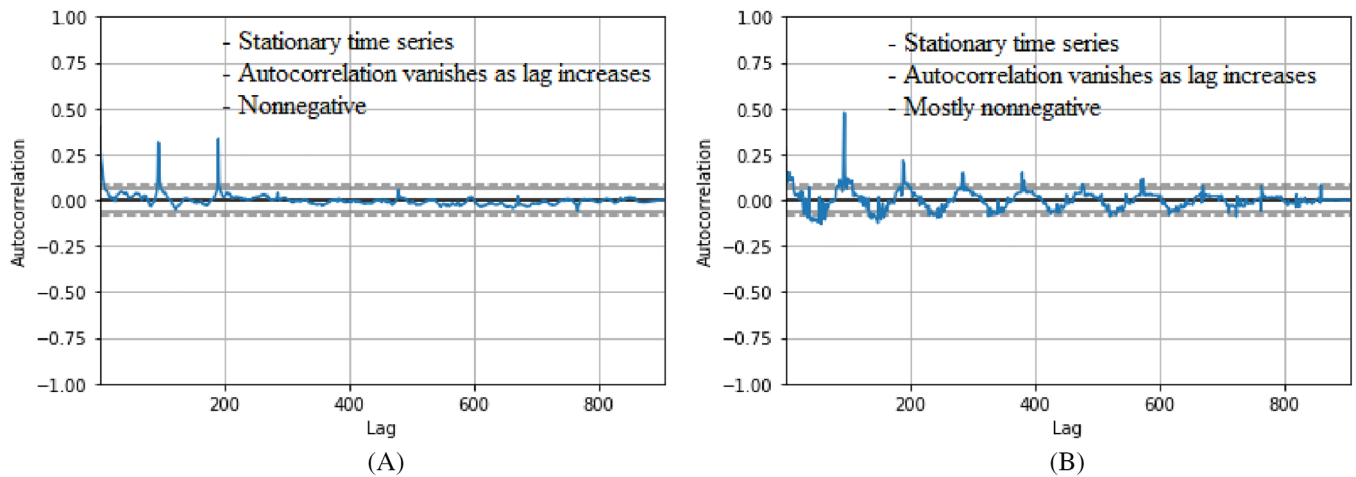


FIGURE 7 Box-Cox transformation. Differenced temperature (A) and differenced pressure (B) autocorrelation functions. The gray lines represents the confidence levels for the autocorrelation test. The textual information presents the main plot findings

$$(1 - \phi_1 z^{-1} - \phi_2 z^{-2})(1 - \Phi_1 z^{-96} - \Phi_2 z^{-192}) \nabla_{96} T_t = \theta_0 + \theta_1 p_t + (1 - \theta z^{-1})(1 - \Theta z^{-96}) \varepsilon_t, \quad (13)$$

where the parameters for the model are: $\phi_1 = 0.8106$, $\phi_2 = -0.0023$, $\Phi_1 = -0.2189$, $\Phi_2 = 0.6046$, $\theta_0 = 2.596 \times 10^{-5}$, $\theta_1 = 0.0064$, $\theta = -0.2748$, and $\Phi = 0.4288$.

- iii. *The optimization algorithms.* There are two possible algorithms to solve the models (Equations 12 and 13), the BFGS and the Nelder–Mead algorithms. In order to evaluate the accuracy and the computational burden of both algorithms, the models for forecasting the pressure and temperature were run and compared with the real data obtained during the injection molding process. From the computational burden point of view, the

BFGS optimization required 1179 and 901 s to fit the temperature and pressure models, respectively, whereas the Nelder–Mead took only 10 and 3 s to fit the temperature and pressure models, respectively. Such high time spent to fit the chosen models through the BFGS method represents an issue during the process operation. Therefore, as it is faster, the Nelder–Mead optimization method is a suitable alternative for this application. This is the method used in this work from now on.

5.3 | Validation of the model

The validation of the proposed model is presented first using different molding conditions by changing the filling time. Second, it was evaluated using a molding process under a deterministic disturbance condition.

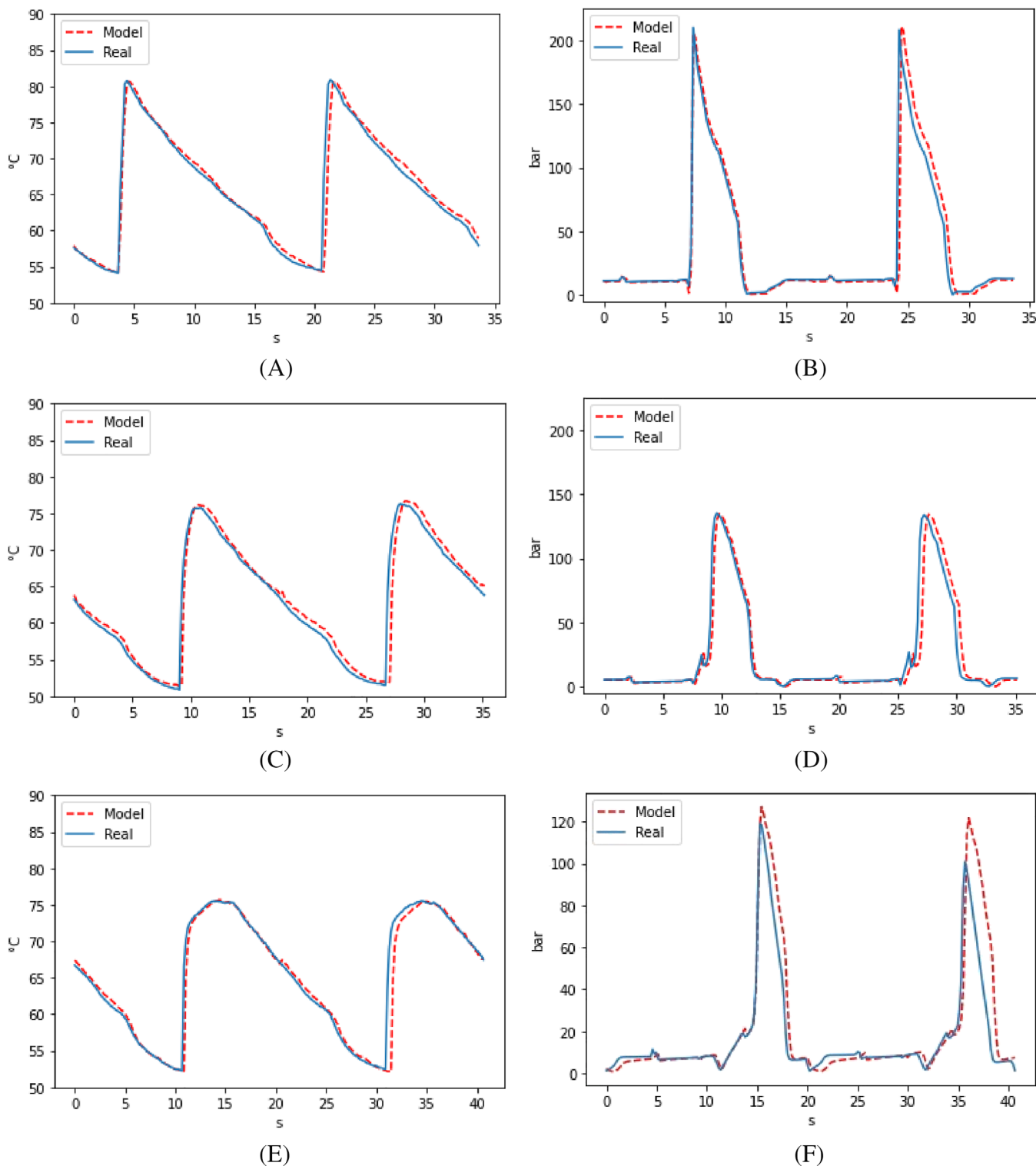


FIGURE 8 Forecasting of the temperature and pressure. (A) Temperature filling time of 0.5 s; (B) pressure filling time of 0.5 s; (C) temperature filling time of 1.0 s; (D) pressure filling time of 1.0 s; (E) temperature filling time of 2.0 s; and (F) pressure filling time of 2.0 s

5.3.1 | Validation under different molding conditions

In this validation, the forecast model SARIMAX (0, 0, 1) × (2, 1, 1) was tested using three different values of

the filling time: 0.5, 1, and 2 s. Figure 8 presents the results of the forecast temperature and pressure for these three molding conditions and their respective real values to show the accuracy of the model. These plots show two injection molding cycles.

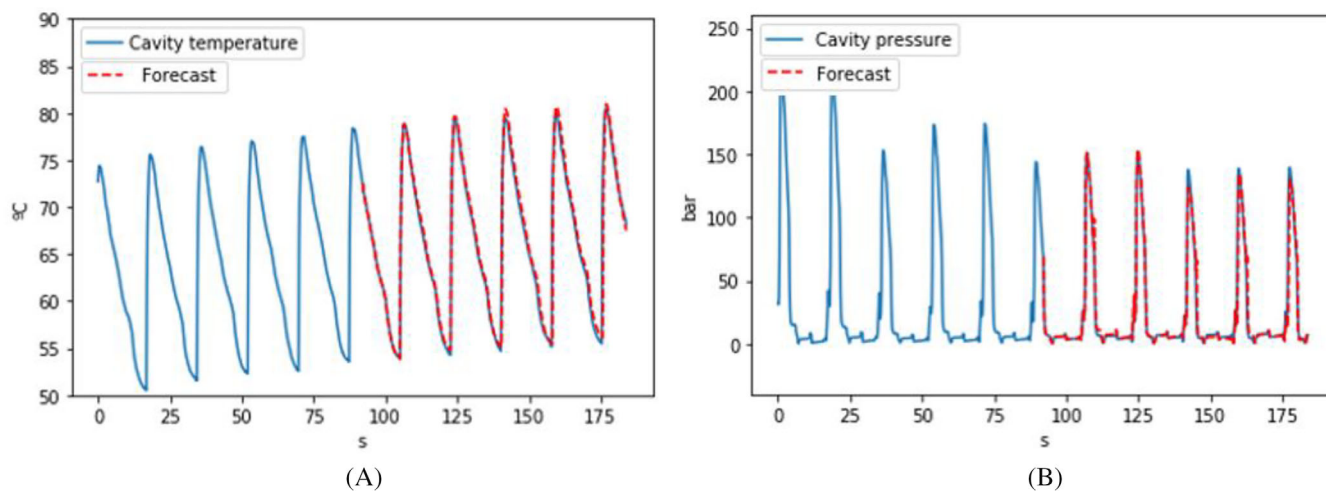


FIGURE 9 Forecasting under deterministic disturbances. (A) Temperature and (B) pressure

Figure 8 shows that the SARIMAX model developed in this work has a very accurate behavior when altering the molding condition by the filling time. The model was designed with a focus on predicting one cycle ahead. However, the second cycle was also forecasted with very high accuracy. The error of the forecasted temperature was very low and can be neglected, and the pressure error was at most 7% for forecasting the first cycle ahead.

5.3.2 | Validation under deterministic disturbances

Using the process parameters with the filling time of 1 s, some deterministic disturbances were induced along a production batch of the plastic part, in order to evaluate the capability of the model to predict transient regimes along a batch production. In an industry, such transient regimes can happen due to undesirable changes in the process parameters (e. g., nozzle temperature and pressure, reciprocating screw velocity, material, humidity).

Figure 9 shows the real temperature and pressure in transient regimes, and the forecasted values obtained from the model. The parameters of the SARIMAX models were estimated using data sampled in five previous cycles to forecast the subsequent ones. These disturbances are incorporated into the process variables' autoregressive dynamics in SARIMAX models, requiring the identification of the process during its operation. SARIMAX $(2, 0, 1) \times (2, 1, 1)_{0.6}$ and SARIMA $(0, 0, 1) \times (2, 1, 1)_{0.6}$ models of the endogenous and exogenous variables, respectively, were fitted and used to make predictions in each injection cycle.

Whereas transient regimes in cavity temperature comprise the occurrence of a trend in the time series, like it is shown in Figure 9A, this does not happen in cavity

pressure time series. This signal exhibits discontinuities between the ejection of one part and the beginning of the next injection cycle. Thereby, the transient behaviors are associated with the variance in the pressure peaks. Then, the proposed model shows the capability of forecasting the molding process under transient regimes, either or not linear trends, with high accuracy. The error on the temperature can be neglected because it is very small, and the maximum error on the pressure was about 8% (but it happened on the third cycle ahead).

The computational burden of the model was significantly low in both validations (under different molding conditions and under deterministic disturbances). Depends on the volume of data, the processing time took between 3 and 12 s, considerably lower than the entire molding cycle (17.6 s).

6 | CONCLUSIONS

This work presents a new statistical model developed to predict the cavity pressure and temperature during any injection molding cycle, throughout a given production batch. The validation of the new model was conducted during a real injection molding process. An injection mold was instrumented with sensors of temperature and pressure, inside its cavities. On the experimental validation the model was trained with data from five injection cycles and the results demonstrated that even using a small number of samples to be trained, the model showed high forecast accuracy. Besides, the validation was also conducted in two different process conditions: first by altering the molding conditions, by the filling time parameter and second by checking the forecasting in a process under deterministic disturbance.

The results shown that the forecast error of temperature was very low, and it can be neglected, and the pressure error was at most 8%. Considering the processing time of the model, at the longer case it took lower than 12 s (it is lower than the entire molding cycle: 17.6 s). Therefore, from the accuracy of the forecasting and computing burden point of view, the proposed model showed to be very efficient.

For the investigated case, the optimization methods Nelder–Mead and BFGS (Broyden–Fletcher–Goldfarb–Shanno) provided very accurate results. However, the Nelder–Mead was significantly faster than the BFGS.

To achieve the proposed model, different implementations and proposals were evaluated. This investigation brings an important scientific contribution about the methods for forecasting molding processes. Considering the complexity of these processes, this investigation showed that the use of seasonal autoregressive operators and the Box–Cox transformations of the process variables can improve the accuracy of the modeling. There is a correlation between cavity pressure and temperature, justifying the use of both of them as covariables. In this manner, the models can forecast the process variables during transient regimes caused by deterministic disturbances, and the forecasts of the exogenous variables can be used on SARIMAX models.

The results demonstrate the potential of the proposed model for managing and monitoring the production of the molding process, under an Industry 4.0 environment. On future works, the model allows the generation of digital twins of the molded parts, considering all the alterations on the parts' properties due to the disturbances that may occur in a batch production during injection molding process. Furthermore, the model lays an important groundwork for a new injection machine control system, either open or closed loop architecture.

ACKNOWLEDGMENTS

The authors thank to the Coordenação de Aperfeiçoamento de Pessoal de Nível Superior (CAPES), to the Conselho Nacional de Desenvolvimento Científico e Tecnológico (CNPq) and to the Fundação de Amparo a Pesquisa e Inovação de Santa Catarina (Fapesc)—project No. 2022TR001437, by the financial support on this research and also to the company Branqs Automation by the assistance on the research project.

DATA AVAILABILITY STATEMENT

The data that support the findings of this study are available from the corresponding author upon reasonable request.

ORCID

Rodolfo Gabriel Pabst  <https://orcid.org/0000-0001-8595-3721>

REFERENCES

- [1] C. Fernandes, A. J. Pontes, J. C. Viana, A. Gaspar-Cunha, *Adv. Polym. Technol.* **2016**, *37*, 429.
- [2] B. H. M. Sadeghi, *J. Mater. Process. Technol.* **2000**, *103*, 411.
- [3] Y. Yang, F. Gao, *Polym. Eng. Sci.* **1999**, *39*, 2042.
- [4] F. Marin, A. F. De Souza, R. G. Pabst, C. H. Ahrens, *Polimeros* **2019**, *29*(3).
- [5] M. R. Kamal, W. I. Patterson, N. Conley, D. Abu Fara, G. Lohfink, *Polym. Eng. Sci.* **1987**, *27*, 1403.
- [6] K. M. Tsai, J. K. Lan, *Int. J. Adv. Manuf. Technol.* **2015**, *79*, 273.
- [7] W. Michaeli, A. Schreiber, *Adv. Polym. Technol.* **2009**, *28*, 65.
- [8] Wang, J. *PVT Properties of Polymers for Injection Molding*. Beijing Institute of Technology, Beijing, China **2012**.
- [9] X. Chen, F. Gao, *Mater. Sci. Eng., A* **2003**, *358*, 205.
- [10] J. S. Nam, C. R. Na, H. H. Jo, J. Y. Song, T. H. Ha, S. W. Lee, *J. Eng. Manuf.* **2016**, *232*, 928.
- [11] J. Wang, Q. Mao, *Adv. Polym. Technol.* **2013**, *32*, 474.
- [12] F. Marin, A. F. De Souza, C. H. Ahrens, *Int. J. Adv. Manuf. Technol.* **2021**, *113*, 1561.
- [13] R. E. S. Bretas, M. A. D'ávila, *Reologia de polímeros fundidos*, 2nd ed., UFSCar, São Carlos **2005**.
- [14] I. Daprà, G. Scarpi, *Meccanica* **2006**, *41*, 501.
- [15] B. Pignon, V. Sobotka, N. Boyard, D. Delaunay, *Int. J. Heat Mass Transfer* **2018**, *118*, 14.
- [16] H. Zhou, Z. Hu, D. Li, in *Computer Modelling for Injection Molding* (Ed: H. Zhou), Wiley, Hoboken **2013**.
- [17] A. Haber, M. R. Kamal, *Polym. Eng. Sci.* **1987**, *27*, 1411.
- [18] C. Zhao, F. Gao, *Polym. Eng. Sci.* **1999**, *39*, 1787.
- [19] S. Haykin, *Neural Networks: A Comprehensive Foundation*, 3rd ed., Prentice Hall, Harlow **2008**.
- [20] P. Zhao, H. Zhou, Y. He, K. Cai, J. Fu, *Int. J. Adv. Manuf. Technol.* **2014**, *72*, 765.
- [21] G. E. P. Box, G. M. Jenkins, G. C. Reinsel, G. M. Ljung, *Time Series Analysis: Forecasting and Control*, 5th ed., Wiley, Hoboken **2016**.
- [22] J. Zhang, P. Zhao, Y. Zhao, J. Huang, N. Xia, J. Fu, *Sens. Actuators, A* **2019**, *1*, 118.
- [23] M. S. Huang, *J. Mater. Process. Technol.* **2007**, *183*, 419.
- [24] R. Zheng, R. I. Tanner, X. J. Fan, *Injection Molding: Integration of Theory and Modelling Methods*, Springer, Sydney **2011**.
- [25] P. J. Brockwell, R. A. Davis, *Time Series: Theory and Methods*, 2nd ed., Springer, New York **1991**.
- [26] G. E. P. Box, D. R. Cox, *J. R. Stat. Soc., Ser. B: Methodol.* **1964**, *26*, 211.

How to cite this article: R. G. Pabst, A. F. de Souza, A. G. Brito, C. H. Ahrens, *Polym. Eng. Sci.* **2022**, *1*. <https://doi.org/10.1002/pen.26166>